Distributed Space-Time Block Codes Achieving Optimal Diversity Function with Linear Receiver

DISTRIBUTED SPACE-TIME BLOCK CODES ACHIEVING OPTIMAL DIVERSITY FUNCTION WITH LINEAR RECEIVER

BY

GONGJIN CHEN, B.Eng.

A THESIS

SUBMITTED TO THE DEPARTMENT OF ELECTRICAL & COMPUTER ENGINEERING

AND THE SCHOOL OF GRADUATE STUDIES

OF MCMASTER UNIVERSITY

IN PARTIAL FULFILMENT OF THE REQUIREMENTS

FOR THE DEGREE OF

MASTER OF APPLIED SCIENCE

Master of Applied Science (2013) McMaster University

(Electrical & Computer Engineering) Hamilton, Ontario, Canada

TITLE:	Distributed Space-Time Block Codes Achieving Optimal Diversity Function with Linear Receiver
AUTHOR:	Gongjin Chen B.Eng., (Electrical Engineering) Beijing Institute of Technology, Beijing, China
SUPERVISOR:	Dr. Kon Max Wong
NUMBER OF PAGES:	xiii, 81

To my parents, Changnuan Liu and Jinyi Chen,

who encouraged and supported me to make a difference.

Abstract

The design and analyses of Space-Time Block Codes (STBC) for both single antenna and two-antenna distributed relay channels are considered in this thesis. Due to the fact that the equivalent channel gains for two-phase relay channels are the product of two channel coefficients, many current STBC designs for Multiple Input Multiple Output (MIMO) channels cannot be implemented to distributed relay channels efficiently. The direct application of Orthogonal Space-Time Block Coding (OSTBC) for MIMO systems to distributed cooperative relay networks makes the equivalent channel matrix for maximum likelihood (ML) detection lose its orthogonality. Hence, a new design that makes the channel matrix be *orthogonally distributed* (OD) for a suboptimal symbol-by-symbol detector (SBSD) is proposed in this thesis. With ODSTBC, an asymptotic symbol error probability (SEP) formula with SBSD is derived, showing the optimal diversity gain function for single antenna distributed relay channels $\frac{\ln^N \rho}{\rho^N}$ is achieved. In addition, two ODSTBC designs for the distributed relay networks are presented, which interestingly renders that SBSD is equivalent to the ML detector. The ODSTBC enjoys both optimal diversity function and low detection complexity. However, the symbol rate of ODSTBC is relatively low in order to maintain the orthogonal conditions. To address this problem, another Alamouti Based Toeplitz Space-Time Block Code (ABTSTBC) for two-antenna distributed

relay channels is proposed. Both the code structure and the equivalent channel matrix has a block Toeplitz structure, whose blocks are the addition and product of two Alamouti matrices, respectively. With the linear SBSD, the optimal diversity function $\frac{\ln^N \rho}{\rho^{2N}}$ is achieved. At the same time, the advantages of low computational complexity and high symbol rate are maintained. Numerical results verify the diversity analyses and indicate competitive error performance to currently available distributed STBC designs with much lower complexity.

Acknowledgements

In these two years of pursuing the degree of Master of Applied Science, the author would like to give his heartfelt thankfulness to his supervisor Dr. Kon Max Wong, whose advisable suggestions, inspiring ideas and virtuous personality have pointed the right way for him in both research and study. Besides, the author wants to thank Dr. Wong for his financial support in pursuing the degree and attending conferences.

In addition, the author really appreciates the guidance and help from Dr. Jian-Kang Zhang, without whom the author cannot progress the research and solve problems easily. Dr. Zhang's proficiency in both signal processing and mathematics greatly promoted the solutions of complex research problems and the publication of the paper in ICASSP 2013.

The author also wants to thank his colleagues in the signal processing group for their support and help in academic problems, the secretaries of the department for their generous help in daily affairs, and technicians for their assistance in computer related inquiries.

Finally, it's the generous and continuous support from the author's parents, Changnuan Liu and Jinyi Chen, that contributes to the author's current achievements.

Notations and Abbreviations

Notations

$\mathbf{A}$	Matrices
$\mathbf{a}$	Column vectors
$(\cdot)^T$	Matrix transpose
$(\cdot)^{-1}$	Matrix inverse
$(\cdot)^\dagger$	Matrix pseudo inverse
$(\cdot)^*$	Matrix complex conjugate
$(\cdot)^H$	Matrix hermitian
$\text{diag}\{\cdot\}$	Diagonal matrix
$\mathbb{E}[\cdot]$	Expectation
$\mathbf{I}_N$	$N \times N$ identity matrix
$H(\cdot)$	Entropy
$I(\cdot)$	Mutual information
$\text{tr}(\cdot)$	Trace of matrices
$\mathbf{0}$	Zero matrices
$\mathbf{A} \succeq \mathbf{B}$	$\mathbf{A}$, $\mathbf{B}$ and $\mathbf{A} - \mathbf{B}$ are all positive semi-definite matrices
$[\mathbf{A}]_{ij}$	The entry in the ith row and jth column

$\otimes$	Kronecker product
$\otimes^n$	n times Kronecker product
$f(x) = \mathcal{O}(g(x))$	$f(x) \leq Cg(x)$, C is a positive constant
δ_{kl}	Kronecker delta: 1, if $k = l$; otherwise 0
$\mathbf{e}_i$	Unit vector, only the ith entry of which is 1
$\|\cdot\|_2$	2-norm of vectors

Abbreviations

ABTSTBC	Alamouti Based Toeplitz Space-Time Block Code
AF	Amplify-and-Forward
BER	Bit Error Rate
CSI	Channel State Information
i.i.d.	Independent and Identically Distributed
ISI	Inter-symbol Interference
LD	Linear Dispersion
MAP	Maximum A Posteriori
MIMO	Multiple Input Multiple Output
MISO	Multiple Input Single Output
ML	Maximum Likelihood
N-D	N Dimensional
ODSBTC	Orthogonally-Distributed Space-Time Block Code
OSTBC	Orthogonal Space-Time Block Code
pdf	Probability Density Function

PEP	Pair-wise Error Probability
PSD	Positive semidefinite
QAM	Quadrature Amplitude Modulation
SBSD	Symbol-by-Symbol Detection
SEP	Symbol Error Probability
SIMO	Single Input Multiple Ouputt
SISO	Single In Single Out
SNR	Signal to Noise Ratio
STBC	Space-Time Block Code

Contents

List of Figures

Chapter 1

Introduction

1.1 Background and Motivation

Installing multiple antennas as in Multiple Input Multiple Output (MIMO) systems is often impractical in mobile communications. Therefore, cooperative diversity has recently been revived [1, 2, 3, 4, 5, 6, 7, 8, 9, 10, 11], in which the in-cell mobile users share the use of their antennas to create a virtual array through distributed transmission and signal processing. Since this arrangement forms a distributed MIMO system, the diversity techniques for the MIMO systems have been naturally extended to such relaying networks for the design of so-called distributed STBC [7, 9, 12]. It is known that among all STBC designs for MIMO systems, Orthogonal STBC [13, 14, 15, 16] is particularly attractive, since they can provide maximum diversity using a linear processing maximum likelihood detector. Hence, a natural question is *whether or not OSTBC can be directly extended to distributed cooperative networks?* Unfortunately, the answer to this question is negative. Unlike in a MIMO system, the channel gain in the relay system is the *product* of two Gaussian random variables. As a result,

the direct application of OSTBC for MIMO systems to distributed cooperative relay networks will make the equivalent channel matrix for ML detection lose its orthogonality. This fact was first realized in [17]. Hence, the researchers in [18, 19] proposed distributed orthogonal STBC designs with the ML receiver. The work of ODSTBC is closely related to those in [18, 19]. However, the idea here is significantly different. We require that the channel matrix is *orthogonally distributed* (OD) for the SBSD rather than the equivalent whitened channel matrix is orthogonal for the ML detector, thereby, avoiding the inverse operation of the noise covariance matrix. Another contribution of this thesis is to derive an asymptotic SEP formula for all ODSTBCs with the SBSD, showing the optimal diversity gain function $\frac{\ln^N \rho}{\rho^N}$ is achieved, which, however, were just verified by computer simulations in [18, 19] without any calculations of SEP. Very interestingly, two kinds of simple ODSTBC designs presented in this paper make the SBSD equivalent to the ML detector.

Although the ODSTBC maintains the orthogonal conditions and achieve the optimal diversity function $\frac{\ln^N \rho}{\rho^N}$ with the two designs and the SBSD, in order to fulfil the orthogonal conditions, the symbol rate is sacrificed greatly. The symbol rate for ODSTBC for 2^n-relay channels is 2^{1-n}, which will decrease dramatically when the number of antennas increases. In order to design a high symbol rate code structure, a two-antenna distributed relay channel model is considered. More antennas will provide more freedom in design and each antenna pair of each relay could fully cooperate with each other, thus offering a better diversity function.

A family of linear Toeplitz Space-Time Block Codes was firstly proposed by Zhang-Liu-Wong in MISO channels [20]. The authors managed to covert the original MISO flat fading channel into a Toeplitz virtual MIMO channel with linear Toeplitz code

structure. The linear Toeplitz code has a symbol rate of $\frac{T}{T+M-1}$ and could achieve full diversity order with linear receivers. Besides, the code also minimizes the worst case PEP with ML detector and approach the optimal diversity-multiplexing tradeoff in independent MISO flat fading systems. Enlightened by this work, Shang-Xia extended the result and designed an overlapped Alamouti code structure based on the Toeplitz structure in MIMO channels [21]. The code could achieve the full diversity with ZF and MMSE receivers and the symbol rate can approach to 1 for any number of transmitter antennas. Based on these papers, a block Toeplitz STBC structure called Alamouti Based Toeplitz Space-Time Block Code (ABTSTBC) for two-antenna distributed relay channels with linear receiver is proposed in this thesis. The code has a block Toeplitz structure, whose 2×2 blocks are the addition of two Alamouti codes. Besides, with some proper manipulations of the channel model, the equivalent channel matrix also has a block Toeplitz structure, whose 2×2 blocks are the product of two Alamouti structures. The coefficients of the 2×2 Alamouti structure product come from the two transmission phases, respectively. With this code structure, the optimal diversity function $\frac{\ln^N \rho}{\rho^{2N}}$ is achieved with linear receivers and the symbol rate of $\frac{K}{K+2N-2}$ is achieved, with K the number of symbols transmitted and N the number of relays. The symbol rate will approach to 1 as the number of transmitted symbols is increased. The structure of the thesis is described in the following section.

1.2 Structure of the Thesis

In this thesis, two code structures for single-antenna distributed relay channels and one for two-antenna distributed relay channels are proposed, respectively. The thesis is arranged as follows. In the first chapter, some background, introduction and

motivation of the topic is provided. In the second chapter, some basic principles and knowledge about MIMO, STBC and relay are introduced. The ODSTBC for single antenna distributed relay channels is derived in the third chapter. In the forth chapter, the STBC for two-antenna distributed relay channels, namely, ABTSTBC is proposed, which could achieve the optimal diversity function with a much higher symbol rate. Simulation results are presented in the fifth chapter and a variety of scenarios are examed in terms of Bit Error Rate (BER) and Symbol Error Probability (SEP). The last chapter concludes the thesis and introduces some prospective future work.

Chapter 2

MIMO, Space-Time Block Codes and Relay

2.1 MIMO Systems

Multiple Input Multiple Output (MIMO) has been recognized as a competitive method to combat channel fading and interference for decades. In MIMO channel systems, multiple antennas are deployed at both the transmitters and receivers, forming a channel with multiple inputs and multiple outputs. MIMO can be used to transmit multiple signal streams simultaneously to improve channel throughput or transmit single signal stream in multiple time slots with multiple antennas to improve the error performance. Therefore, the MIMO system could provide both diversity gain and multiplexing gain. Diversity is a term to describe the number of independent copies of signals transmitted through different fading channels, while multiplexing is used to describe the state that multiple signals are transmitted through shared medium.

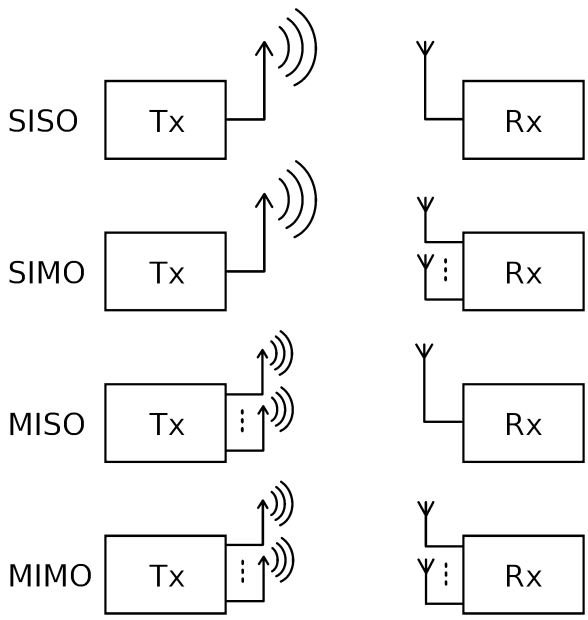

Figure 2.1: Common channel models

2.1.1 General MIMO Channel Model

The MIMO channel can be described with the Figure 2.1. Multiple antennas are equipped at both transmitter and receiver, which can be regarded as an extension of SISO, MISO and SIMO channels. For general channel models, M transmitting antennas and N receiving antennas are deployed at the transmitter and receiver, respectively. The transmission can be depicted by the following linear matrix equation.

$$\begin{bmatrix} y_1 \\ \vdots \\ y_N \end{bmatrix} = \begin{bmatrix} h_{11} & \cdots & h_{1M} \\ \vdots & \ddots & \vdots \\ h_{N1} & \cdots & h_{NM} \end{bmatrix} \begin{bmatrix} x_1 \\ \vdots \\ x_M \end{bmatrix} + \begin{bmatrix} n_1 \\ \vdots \\ n_N \end{bmatrix} \tag{2.1}$$

which can also be represented in the compact form as $\mathbf{y} = \mathbf{H}\mathbf{x} + \mathbf{n}$. $\mathbf{x}$ is the $M \times 1$ transmitting vector, $\mathbf{y}$ is the $N \times 1$ receiving vector and $\mathbf{n}$ is the $N \times 1$ noise vector.

h_{ij} denotes the channel gain from the jth transmitting antenna to the ith receiving antenna and the channel coefficients are usually modeled as zero-mean circular symmetric complex Gaussian variables with unit variance.The noise variables are also described as zero-mean circular symmetric complex Gaussian variables.

2.1.2 Detection Methods

The general MIMO system model is described in the linear matrix equation (2.1), or the following equation for simplicity.

$$\mathbf{y} = \mathbf{H}\mathbf{x} + \mathbf{n} \tag{2.2}$$

The symbol vector transmitted from the source $\mathbf{x}$ is multiplied by the channel coefficients matrix and contaminated by the noise vector $\mathbf{n}$. In order to recover the symbols and eliminate the Inter-Symbol Interference (ISI) at the destination, many linear and nonlinear detection methods have been devised [29, 30, 31, 32].

Maximum Likelihood Detection

If the symbols transmitted are randomly selected from a certain constellation with equal probability, the optimal detection method is the Maximum Likelihood detection, which minimizes the distance between the transmitted vector and the estimated one. From the point of estimation theory, the ML detection minimizes the probability of making a wrong decision, which is equivalent to the Maximum A Posteriori (MAP) when the symbols are equally likely chosen. Assuming that the noise vector is zero-mean circular symmetric complex multivariate Gaussian distributed with the covariance matrix $\mathbf{\Sigma}$, the conditional probability of making a decision $\mathbf{y}$ given the

transmitted vector $\mathbf{x}$ is [38]

$$p(\mathbf{y}|\mathbf{x}) = \frac{1}{(\pi)^M|\mathbf{\Sigma}|}\exp\left(-(\mathbf{y}-\mathbf{H}\mathbf{x})^H\mathbf{\Sigma}^{-1}(\mathbf{y}-\mathbf{H}\mathbf{x})\right). \tag{2.3}$$

In order to minimize the error probability, we need to find $\mathbf{y}$ that maximizes the $p(\mathbf{y}|\mathbf{x})$, which is equivalent to finding the $\mathbf{y}$ minimizing the distance between $\mathbf{y}$ and $\mathbf{H}\mathbf{x}$.

$$\min_{\mathbf{y}} \quad (\mathbf{y}-\mathbf{H}\mathbf{x})^H\mathbf{\Sigma}^{-1}(\mathbf{y}-\mathbf{H}\mathbf{x}) \tag{2.4}$$

The ML detection can be solved by numerical computations efficiently.

Linear Receivers

Considering the complexity of ML detection, linear receivers are preferred in circumstances where computation ability is limited or the time delay is critical. There are two linear receivers that are commonly used: Zero-Forcing (ZF) receiver and Minimum Mean Square Error (MMSE) receiver. Assuming the receiver is denoted as $\mathbf{G}$, the estimated symbols can be denoted as

$$\hat{\mathbf{x}} = \mathbf{G}\mathbf{y} = \mathbf{G}\mathbf{H}\mathbf{x} + \mathbf{G}\mathbf{n} \tag{2.5}$$

Zero-Forcing Receiver

The ZF receiver makes the symbols in the vector $\mathbf{x}$ interference-free by requiring the product of $\mathbf{G}$ and $\mathbf{H}$ equal to identity matrix, i.e. $\mathbf{G}\mathbf{H} = \mathbf{I}$. However, the noise will be amplified intensely in some sub-channels when the original channel gain is very small. Since there is no interference between symbols, the mean square error (MSE)

is just the power of the noise . In the optimization point of view, the ZF receiver can be resolved by solving the following problem.

$$\begin{aligned} \mathbf{G}_{\mathrm{ZF}} &= \arg\min_{\mathbf{G}} \mathbb{E}\left[\|\mathbf{G}\mathbf{n}\|_2^2\right] \\ \text{subject to} \quad & \mathbf{G}\mathbf{H} = \mathbf{I} \end{aligned} \tag{2.6}$$

From the detection point of view, ZF receiver is the pseudo inverse of the whitened channel matrix. Therefore, ZF receiver $\mathbf{G}$ can be described by the product of two parts, i.e. $\mathbf{G} = \tilde{\mathbf{G}}\mathbf{W}$, where $\mathbf{W}$ is used to whiten the channel and $\tilde{\mathbf{G}}$ is the pseudo inverse of the whitened channel matrix. Since the covariance matrix of noise is $\mathbf{\Sigma}$, the whiten matrix $\mathbf{W} = \mathbf{\Sigma}^{-\frac{1}{2}}$. Multiplying $\mathbf{W}$ with (2.2), we have a whitened channel model.

$$\tilde{\mathbf{y}} = \mathbf{\Sigma}^{-\frac{1}{2}}\mathbf{H}\mathbf{s} + \tilde{\mathbf{n}}, \tag{2.7}$$

where $\mathbb{E}[\tilde{\mathbf{n}}\tilde{\mathbf{n}}^H] = \mathbf{I}$. The receiver $\tilde{\mathbf{G}}$ is the pseudo inverse of the equivalent channel matrix $\mathbf{\Sigma}^{-\frac{1}{2}}\mathbf{H}$. Therefore, the interference-free linear receiver is

$$\tilde{\mathbf{G}} = (\mathbf{\Sigma}^{-\frac{1}{2}}\mathbf{H})^{\dagger} = (\mathbf{H}^H\mathbf{\Sigma}^{-1}\mathbf{H})^{-1}\mathbf{H}^H\mathbf{\Sigma}^{-\frac{1}{2}} \tag{2.8}$$

MMSE Receiver

While the ZF receiver eliminates the interference but increases some noise potentially, the MMSE receiver provides a compromise between interference and noise. The MMSE receiver minimizes the MSE of the transmitted signal and the estimated one.

$$\mathbf{G}_{\mathrm{MMSE}} = \arg\min_{\mathbf{G}} \mathbb{E}\left[\|\mathbf{x} - \hat{\mathbf{x}}\|_2^2\right] \tag{2.9}$$

From the detection point of view, the MMSE receiver can be solved easily with the orthogonality principle [33], namely, $\mathbb{E}[(\hat{\mathbf{x}} - \mathbf{x})\mathbf{y}^H] = \mathbf{G}\mathbf{R}_{yy} - \mathbf{R}_{xy} = 0$, where $\mathbf{R}_{yy} = \mathbb{E}[\mathbf{y}\mathbf{y}^H]$ and $\mathbf{R}_{xy} = \mathbb{E}[\mathbf{x}\mathbf{y}^H]$ are the covariance matrix of $\mathbf{y}$ and cross covariance matrix of $\mathbf{x}$ and $\mathbf{y}$, respectively. With this condition, the MMSE receiver can be derived as

$$\mathbf{G}_{\text{MMSE}} = \mathbf{R}_{xx}\mathbf{H}^H(\mathbf{H}\mathbf{R}_{xx}\mathbf{H}^H + \mathbf{\Sigma})^{-1} \tag{2.10}$$

An alternative expression is also provided in (2.11). The equivalence of (2.10) and (2.11) can be verified by post-multiplying by $(\mathbf{H}\mathbf{R}_{xx}\mathbf{H}^H + \mathbf{\Sigma})$ and then pre-multiplying by $(\mathbf{H}^H\mathbf{\Sigma}^{-1}\mathbf{H} + \mathbf{R}_{xx}^{-1})$.

$$\mathbf{G}_{\text{MMSE}} = (\mathbf{H}^H\mathbf{\Sigma}^{-1}\mathbf{H} + \mathbf{R}_{xx}^{-1})^{-1}\mathbf{H}^H\mathbf{\Sigma}^{-1}, \tag{2.11}$$

where $\mathbf{R}_{xx} = \mathbb{E}[\mathbf{x}\mathbf{x}^H]$ is the covariance matrix of $\mathbf{x}$. As we can see from the expression above, when the SNR is sufficiently large, the term $\mathbf{R}_{xx}^{-1}$ is negligible compared to the first term in the parentheses. The MMSE receiver converges to the ZF receiver as SNR increases to infinity. Therefore, when SNR is sufficiently high, ZF receiver is usually preferred due to its simplicity and comparable performance to MMSE receiver. When SNR is low, MMSE is preferred as it can handle the noise more effectively.

2.1.3 Capacity of MIMO Channels

The Shannon channel capacity is the maximum information rate that can be reliably transmitted. In MIMO channels, depending on whether CSI is known to both transmitter and receiver, or only known to the receiver, we can evaluate the maximum mutual information in the following cases:

Case 1: CSI known to both transmitter and receiver: Waterfilling method [34]

When CSI are known to both transmitter and receiver, the channel capacity is the maximum mutual information available.

$$C = \max_{p(\mathbf{x})} I(\mathbf{X};\mathbf{Y}) = \max_{p(\mathbf{x})} \left[H(\mathbf{Y}) - H(\mathbf{Y}|\mathbf{X})\right], \tag{2.12}$$

where $H(\cdot)$ is the entropy and $I(\cdot)$ is the mutual information. If we denote the covariance matrix of transmitted symbols as $\mathbf{R}_{xx}$, the covariance matrix of the received signals is thus

$$\mathbf{R}_{yy} = \mathbb{E}\left[\mathbf{y}\mathbf{y}^H\right] = \mathbf{H}\mathbf{R}_{xx}\mathbf{H}^H + \mathbf{I}_N \tag{2.13}$$

The mutual information of transmitter and receiver can be calculated as [25, 26], when the input is assumed to be Gaussian,

$$I(\mathbf{X};\mathbf{Y}) = \log_2 \det\left[\mathbf{I}_N + \mathbf{H}\mathbf{R}_{xx}\mathbf{H}^H\right] \tag{2.14}$$

Therefore, the channel capacity C is the maximum mutual information subject to the transmitting power constraint:

$$C \triangleq \max_{\mathrm{tr}(\mathbf{R}_{\mathrm{xx}})\leq 1} \log_2 \det\left[\mathbf{I}_N + \mathbf{H}\mathbf{R}_{xx}\mathbf{H}^H\right], \tag{2.15}$$

assuming that the transmitted power is 1. With some matrix manipulations, the maximum capacity can be obtained through water filling technique [35]

$$C = \log_2\left(r^{-r}\left(1 + \sum_{j=1}^{r} \lambda_j^{-1}\right)\prod_{j=1}^{r}\lambda_j\right), \tag{2.16}$$

where r is the maximum integer satisfying $r < \lambda_r \left(1 + \sum_{j=1}^{r} \lambda_j^{-1}\right)$ and λ_j the the jth maximum eigen value of $\mathbf{H}^H\mathbf{H}$. The corresponding power allocation to achieve the the capacity is

$$P_i = r^{-1}\left(1 + \sum_{j=1}^{r} \lambda_j^{-1}\right) - \lambda_i^{-1}, \tag{2.17}$$

where P_i corresponds to the ith largest eigen value of $\mathbf{R}_{xx}$.

Case 2: CSI unknown at transmitter [26]

When CSI is not available at the transmitter, the transmitter cannot dynamically allocate the power according to the channel gains, as is shown in the previous instance. Therefore, a reasonable method is to calculate the maximum mutual information by taking the expectation with respect to the random channel matrix $\mathbf{H}$. The capacity can be described with the following optimization problem:

$$\max_{\mathrm{tr}(\mathbf{R}_{\mathrm{xx}})\leq \mathrm{P}} \mathbb{E}_{\mathbf{H}}\left[\log_2 \det\left(\mathbf{I}_N + \mathbf{H}\mathbf{R}_{xx}\mathbf{H}^H\right)\right] \tag{2.18}$$

If we represent the signal covariance matrix as $\mathbf{R}_{xx} = \mathbf{V}\mathbf{D}\mathbf{V}^H$ and $\mathbf{D} = \mathrm{diag}(\mathrm{d}_1, \cdots, \mathrm{d}_\mathrm{M})$, the matrix $\mathbf{HV}$ will have the same Gaussian distribution as $\mathbf{H}$. Therefore,

$$\begin{aligned}\psi(\mathbf{R}_{xx}) &= \mathbb{E}_{\mathbf{H}}\left[\log_2 \det\left(\mathbf{I}_N + \mathbf{H}\mathbf{R}_{xx}\mathbf{H}^H\right)\right] \\ &= \mathbb{E}_{\mathbf{HV}}\left[\log_2 \det\left(\mathbf{I}_N + \mathbf{HVD}(\mathbf{HV})^H\right)\right] \\ &= \mathbb{E}_{\mathbf{H}}\left[\log_2 \det\left(\mathbf{I}_N + \mathbf{H}\mathbf{D}\mathbf{H}^H\right)\right]\end{aligned} \tag{2.19}$$

when deriving the equations above, we make the assumptions that the channel coefficients in $\mathbf{H}$ are *i.i.d.* Gaussian Distributed. Therefore, multiplying $\mathbf{H}$ by $\mathbf{V}$ will not affect the original distribution of $\mathbf{H}$. If we define $\tilde{\mathbf{D}} = \frac{1}{K}\sum_i \boldsymbol{\Pi_i} \boldsymbol{D} \boldsymbol{\Pi}_i^H$, where $\boldsymbol{\Pi}_i$ are the permutation matrices and K is the number of permutation matrices, then the

expression above can be translated into

$$\begin{aligned}
\psi(\mathbf{D}) &= \frac{1}{K}\sum_i \mathbb{E}_{\mathbf{H}}\left[\log_2 \det\left(\mathbf{I}_N + \mathbf{H}\mathbf{\Pi}_i\mathbf{D}(\mathbf{H}\mathbf{\Pi}_i)^H\right)\right] \\
&= \mathbb{E}_{\mathbf{H}}\left[\frac{1}{K}\sum_i \log_2 \det\left(\mathbf{I}_N + \mathbf{H}\mathbf{\Pi}_i\mathbf{D}(\mathbf{H}\mathbf{\Pi}_i)^H\right)\right] \\
&\leq \mathbb{E}_{\mathbf{H}}\left[\log_2 \det\left(\mathbf{I}_N + \mathbf{H}\left(\frac{1}{K}\sum_i \mathbf{\Pi}_i\mathbf{D}\mathbf{\Pi}_i\right)\mathbf{H}^H\right)\right] \\
&= \mathbb{E}_{\mathbf{H}}\left[\log_2 \det\left(\mathbf{I}_N + \mathbf{H}\tilde{\mathbf{D}}\mathbf{H}^H\right)\right] \\
&= \mathbb{E}_{\mathbf{H}}\left[\log_2 \det\left(\mathbf{I}_N + \frac{P}{M}\mathbf{H}\mathbf{H}^H\right)\right]
\end{aligned} \tag{2.20}$$

The inequality is due to the concaveness of the function $\log_2 \det(\mathbf{I} + \mathbf{X})$ in terms of $\mathbf{X}$. Therefore, when the power is equally allocated to each antenna, the mutual information is maximized, which is the channel capacity when CSI is only known to the receiver.

2.2 Space-Time Block Codes

Space-Time Block Codes (STBC) were invented more than a decade ago and are still good solutions for wireless communications to combat channel fading and interference [7, 12, 13, 14, 15, 36]. In typical Space-Time Block Code models, multiple antennas are employed to transmit multiple copies of symbols strategically over a range of time slots. Then, the receiver can combine the symbols from different physical channels, with single antenna or multiple antennas, to get a better error performance. The improvement in error performance can be described with the term diversity, which denotes the number of independent copies of signals transmitted through independent

fading channels. In typical settings, if M transmitting antennas are deployed, N receiving antennas are used for detection and the symbols are transmitted over a range of T time slots, the STBC could be represented as $T \times M$ matrix (2.21), the (t, m)th entry of the matrix denotes the symbols transmitted in the tth time slots with the mth transmit antenna.

$$\begin{array}{c} \\ \text{time slots} \end{array} \overset{\text{transmit antennas} \longrightarrow}{\begin{array}{|c|} \hline \\ \\ \\ \\ \hline \end{array}} \begin{bmatrix} x_{11} & x_{12} & \cdots & x_{1N} \\ x_{21} & x_{22} & \cdots & x_{2N} \\ \vdots & \vdots & \ddots & \vdots \\ x_{T1} & x_{T2} & \cdots & x_{TN} \end{bmatrix} \tag{2.21}$$

The transmission process can be denoted with the following linear matrix equation, $\mathbf{Y} = \mathbf{XH} + \mathcal{N}$.

$$\underbrace{\begin{bmatrix} y_{11} & \cdots & h_{1N} \\ \vdots & \ddots & \vdots \\ h_{T1} & \cdots & h_{TN} \end{bmatrix}}_{\mathbf{Y}} = \underbrace{\begin{bmatrix} x_{11} & \cdots & x_{1M} \\ \vdots & \ddots & \vdots \\ x_{T1} & \cdots & x_{TM} \end{bmatrix}}_{\mathbf{X}} \underbrace{\begin{bmatrix} h_{11} & \cdots & h_{1N} \\ \vdots & \ddots & \vdots \\ h_{M1} & \cdots & h_{MN} \end{bmatrix}}_{\mathbf{H}} + \underbrace{\begin{bmatrix} n_{11} & \cdots & h_{1N} \\ \vdots & \ddots & \vdots \\ n_{T1} & \cdots & n_{TN} \end{bmatrix}}_{\mathcal{N}} \tag{2.22}$$

2.2.1 Alamouti Code

Among all kinds of STBC, a simple and efficient orthogonal code structure was Alamouti Code, proposed by Siavash Alamouti [13]. The code structure is designed as Alamouti Code and the equivalent channel matrix also forms an Alamouti structure

when properly transformed. The transmitter uses two transmitting antennas, while the receiver uses single antenna for detection. The transmission is finished in two time slots. In the first slot, two different symbols s_1 and s_2 are transmitted with the first and the second antenna, respectively. In the second time slot, the first antenna transmits $-s_2^*$, while the second antenna transmits s_1^*.

The code structure can be described with the following 2×2 matrix.

$$\mathbf{X} = \begin{bmatrix} s_1 & s_2 \\ -s_2^* & s_1^* \end{bmatrix} \tag{2.23}$$

Therefore, the transmission can be represented as $\mathbf{y} = \mathbf{X}\mathbf{h} + \mathbf{n}$:

$$\begin{bmatrix} y_1 \\ y_2 \end{bmatrix} = \begin{bmatrix} s_1 & s_2 \\ -s_2^* & s_1^* \end{bmatrix} \underbrace{\begin{bmatrix} h_1 \\ h_2 \end{bmatrix}}_{\mathbf{h}} + \begin{bmatrix} n_1 \\ n_2 \end{bmatrix}, \tag{2.24}$$

where we denote the noise covariance matrix as $\mathbf{\Sigma} = \mathbb{E}[\mathbf{n}\mathbf{n}^H] = \sigma^2\mathbf{I}$. In order to show the diversity, we manipulate the linear matrix equation above and transform into the following form, by taking the conjugate of the second equation in the linear matrix equation.

$$\begin{bmatrix} y_1 \\ y_2^* \end{bmatrix} = \underbrace{\begin{bmatrix} h_1 & h_2 \\ h_2^* & -h_1^* \end{bmatrix}}_{\boldsymbol{\mathcal{H}}} \begin{bmatrix} s_1 \\ s_2 \end{bmatrix} + \begin{bmatrix} n_1 \\ n_2^* \end{bmatrix}. \tag{2.25}$$

$\boldsymbol{\mathcal{H}}$ is also an Alamouti structure and we can easily verify that $\boldsymbol{\mathcal{H}}\boldsymbol{\mathcal{H}}^H = \boldsymbol{\mathcal{H}}^H\boldsymbol{\mathcal{H}} = \|\mathbf{h}\|^2\mathbf{I}$. When at least one channel gain $h_i, i = 1, 2$ is nonzero, the channel matrix $\boldsymbol{\mathcal{H}}$ is unitary up to a scale, thus full rank. Therefore, if we multiple (2.25) with $\boldsymbol{\mathcal{H}}^H$, the

symbols s_1 and s_2 can be decoded separately since the noise is still white.

$$\tilde{\mathbf{y}} = \mathcal{H}^H \begin{bmatrix} y_1 \\ y_2^* \end{bmatrix} = \|\mathbf{h}\|^2 \begin{bmatrix} s_1 \\ s_2 \end{bmatrix} + \tilde{\mathbf{n}}. \tag{2.26}$$

where $\tilde{\mathbf{n}} = \mathcal{H}^H[n_1\ n_2^*]^T$. The new noise vector $\tilde{\mathbf{n}}$ is still white, whose covariance matrix is $\sigma^2\|\mathbf{h}\|^2\mathbf{I}$. Therefore, the two symbols $\tilde{y}_1$ and $\tilde{y}_2$ can be detected separately: $\tilde{y}_i = \|\mathbf{h}\|^2 s_i + \tilde{n}_i$, $i = 1, 2$. The SNR for each symbol is $\|\mathbf{h}\|^2 E_s/E_n = (|h_1|^2 + |h_2|^2)E_s/\sigma^2$. With Alamouti code structure, the detection processing is extremely simple and the symbols can be decoded symbol by symbol.

2.2.2 Linear Dispersion Code

When the 2×1 MISO channel is used, the Alamouti Code structure can achieve full diversity and simple detection complexity. When more transmitting antennas are deployed, various code structures have been proposed, but many of them suffer from decoding complexities or performance degradation in the circumstances of high rate and multiple antennas [13, 14]. A family of linear codes was proposed by Hassibi and Hochwald called Linear Dispersion (LD) codes [37] , which maintains linear complexity.

Suppose the transmission channel is equipped with M transmitting antennas and N receiving antennas. In the t-th ($t \leq T$) slot, an $M \times 1$ vector is transmitted and the mth entry of the vector is the symbol transmitted with the mth antenna. Therefore, for T transmission time slots, the T $M \times 1$ vectors form a $T \times M$ matrix, which can be represented as

$$\mathbf{X}(\mathbf{s}) = \sum_{k=1}^{K} \mathbf{A}_k s_k + \sum_{k=1}^{K} \mathbf{B}_k s_k^*, \tag{2.27}$$

where $\mathbf{s} \in \mathbb{C}^{K\times 1}$ is the $K \times 1$ symbol vector transmitted, $\mathbf{s} = [s_1, s_2, \cdots, s_K]^T$, and $\mathbf{A}_k \in \mathbb{C}^{T\times M}$ and $\mathbf{B}_k \in \mathbb{C}^{T\times M}$ are $T \times M$ matrices determined by certaind design criteria. The symbols transmitted are randomly selected from a certain constellation and the symbol rate for this structure is K/T. From the structure (2.27), we can easily verify that the code structure is linear with regard to the real and imaginary parts of the symbols, respectively.

At the receiver, the signal can be expressed as

$$\mathbf{Y} = \sqrt{\frac{\rho}{M}}\mathbf{X}(\mathbf{s})\mathbf{H} + \mathbf{\Xi}, \tag{2.28}$$

where ρ is the Signal to Noise Ratio (SNR) per receiving antenna, $\mathbf{H} \in \mathbb{C}^{M\times N}$ is the channel matrix, and $\mathbf{Y} \in \mathbb{C}^{T\times N}$ and $\mathbf{\Xi} \in \mathbb{C}^{T\times N}$ are the receiver's symbol matrix and noise matrix, respectively. In order to analyze the diversity and coding of the LD code, we make the following assumptions.

- The symbols are randomly selected from a certain constellation with equal probability and the power is normalized to 1, i.e., $\mathbb{E}[\mathbf{s}\mathbf{s}^H] = \mathbf{I}_K$
- The channel coefficients h_{mn} are assumed to be zero-mean circular symmetric complex white Gaussian random variables with unit variance
- The channel coefficients remain unchanged within the T time slots of each transmission process
- The noise variable is assumed to be *i.i.d.* zero-mean circular symmetric complex Gaussian random variables

- Full channel state information (CSI) is available at the receiver and ML detection is employed

With these assumptions, we can evaluate the Pair-wise Error Probability (PEP) with a specific channel realization [38]:

$$P(\mathbf{s} \to \mathbf{s}'|\mathbf{H}) = Q\left(\frac{d(\mathbf{s},\mathbf{s}')}{\sqrt{2}}\right), \qquad \mathbf{s} \neq \mathbf{s}' \tag{2.29}$$

where $Q(\cdot)$ is the Q function, i.e. $Q(x) = \frac{1}{\sqrt{2\pi}}\int_x^{+\infty}\exp(-t^2/2)dt$, and $d(\mathbf{s},\mathbf{s}')$ is the distance between the transmitted symbol and detected one denoted by

$$d^2(\mathbf{s},\mathbf{s}') = \frac{\rho}{M}\mathrm{tr}\left[\mathbf{H}^{\mathrm{H}}\mathbf{\Sigma}^{\mathrm{H}}((\mathrm{s}-\mathrm{s})')\mathbf{\Sigma}((\mathrm{s}-\mathrm{s})')\mathbf{H}\right]. \tag{2.30}$$

Using the alternative expression of the Q function [33]

$$Q(x) = \frac{1}{\pi}\int_0^{\frac{\pi}{2}}\exp\left(-\frac{x^2}{2\sin^2\theta}\right)d\theta \tag{2.31}$$

and the property of vectorization, i.e. $\mathrm{tr}(\mathbf{X}^{\mathrm{H}}\mathbf{X}) = \mathrm{vec}(\mathbf{H})^{\mathrm{H}}\mathrm{vec}(\mathbf{H})$ and $\mathrm{vec}(\mathbf{XYZ}) = (\mathbf{Z}^{\mathrm{T}}\otimes\mathbf{X})\mathrm{vec}(\mathbf{Y})$, we can transform (2.30) into

$$d^2(\mathbf{s},\mathbf{s}') = \frac{\rho}{M}\mathrm{vec}(\mathbf{H})^{\mathrm{H}}\left(\mathbf{I}_{\mathrm{N}}\otimes\mathbf{\Sigma}^{\mathrm{H}}(\mathbf{e})\mathbf{\Sigma}(\mathbf{e})\right)\mathrm{vec}(\mathbf{H}), \tag{2.32}$$

where $\mathbf{e} = \mathbf{s} - \mathbf{s}'$ is the error vector. By combining (2.29), (2.31) and (2.32), and taking the expectation with respect to the random vector $\mathrm{vec}(\mathbf{H})$, the average PEP

with ML detection can be reformulated as

$$P(\mathbf{s} \to \mathbf{s}') = \frac{1}{\pi} \int_0^{\pi/2} \frac{d\theta}{\det\left(\mathbf{I}_M + \frac{\rho}{4M \sin^2\theta} \mathbf{\Sigma}^H(\mathbf{e}) \mathbf{\Sigma}(\mathbf{e})\right)^N} \tag{2.33}$$

By applying the Chernoff bound (treat $\sin^2\theta = 1$, since $|\sin\theta| \leq 1$), the PEP can be upper bounded by

$$P(\mathbf{s} \to \mathbf{s}') \leq \frac{1}{2} \det\left(\mathbf{I}_M + \frac{\rho}{4M \sin^2\theta} \mathbf{\Sigma}^H(\mathbf{e}) \mathbf{\Sigma}(\mathbf{e})\right)^{-N} \tag{2.34}$$

The Chernoff bound in the equation above serves as a guidance for the code design, which will be illustrated in the next subsection. The determinant can be further upper bounded by

$$\begin{aligned} & \det\left(\mathbf{I}_M + \frac{\rho}{4M \sin^2\theta} \mathbf{\Sigma}^H(\mathbf{e}) \mathbf{\Sigma}(\mathbf{e})\right)^{-N} \\ \leq & \prod_{m=1}^{M} \left(1 + \frac{\rho}{4M} \cdot \lambda_m\right)^{-N} \\ \leq & \prod_{m=1}^{r} \left(\frac{\rho}{4M} \cdot \lambda_m\right)^{-N} \\ = & \left(\frac{\rho}{4M}\right)^{-rN} \left(\prod_{m=1}^{r} \lambda_m\right)^{-N}, \end{aligned} \tag{2.35}$$

where $r \leq M$ is the rank of $\mathbf{\Sigma}^H(\mathbf{e})\mathbf{\Sigma}(\mathbf{e})$ and $\lambda_m, m = 1, \cdots, r$, are the first r nonzero eigenvalues in descending order. Therefore, with the general code structures, the achieved diversity order is rN. In order to design the codes such that the PEP upper bound is low and the diversity order is high, two criteria are explored in the next subsection.

2.2.3 Rank Criterion and Determinant Criterion

There are many criteria to design Space-Time Block Codes, among which there are two features we consider most: diversity gain and coding gain. In order to design codes maximizing these two aspects, we have the following two design criteria.

- The Rank Criterion

  The upper bound of the PEP can be represented in the expression (2.34) and the determinant can be simplified as (2.35). Therefore, it's easy to see that the diversity order of Space-Time Block Codes is rN, where r is the rank of $\mathbf{\Sigma}^H(\mathbf{e})\mathbf{\Sigma}(\mathbf{e})$. In order to have a high diversity order, the codes designed should have a higher r, such that the PEP will diminish faster as SNR increases. Since r is the rank of the error matrix $\mathbf{\Sigma}^H(\mathbf{e})\mathbf{\Sigma}(\mathbf{e})$, which is a $M \times M$ matrix. Therefore, the optimal codes for maximum diversity, MN, should have a full rank error matrix, i.e. full rank $\mathbf{\Sigma}^H(\mathbf{e})\mathbf{\Sigma}(\mathbf{e})$ as long as $\mathbf{e}$ is a nonzero vector. In designing Space-Time Block Codes, in order to maximize the diversity order, we always want to maximize the rank of the error matrix $\mathbf{\Sigma}^H(\mathbf{e})\mathbf{\Sigma}(\mathbf{e})$.

- The Determinant Criterion

  The second term in (2.35) consists of the product of nonzero eigenvalues of the error matrix $\mathbf{\Sigma}^H(\mathbf{e})\mathbf{\Sigma}(\mathbf{e})$. In order to make the PEP decrease at a faster pace as SNR increases, we always want the product of nonzero eigenvalues to be larger. Among different realization of vector pairs $\{\mathbf{s}, \mathbf{s}'\}$, the minimum value of the product $(\prod_{m=1}^{r} \lambda_m)^r$ dominate the overall PEP performance. Thus the worst case of this term should be maximized when designing the code structures.

2.2.4 Orthogonal STBC

While the STBC can vary in different forms and complexities, a family of STBC commonly used is Orthogonal STBC (OSTBC). OSTBC has an extra condition of orthogonality $\mathbf{X}^H\mathbf{X} = \|\mathbf{x}\|^2\mathbf{I}$, where $\mathbf{X}$ is the STBC structure and $\mathbf{x}$ is the symbol vector. In $M \times 1$ MISO channels, the channel model can be represented as

$$\mathbf{Y} = \mathbf{X}(\mathbf{s})\mathbf{h} + \mathbf{n}, \tag{2.36}$$

where $\mathbf{h} \in \mathbb{C}^M$ is the channel coefficients vector. If OSTBC is implemented in MIMO channels, the channel model is exactly the same as (2.28). MISO channel model is illustrated here for simplicity.

If LD coding scheme is implemented to transmit K symbols, i.e. $\mathbf{X}(\mathbf{s}) = \sum_{k=1}^{K} \mathbf{A}_k s_k + \sum_{k=1}^{K} \mathbf{B}_k s_k^*$, the product $\mathbf{X}(\mathbf{s})\mathbf{h}$ can be rewritten by exacting the symbols out of the code structure.

$$\mathbf{X}(\mathbf{s})\mathbf{h} = (\mathbf{A}_1\mathbf{h}, \mathbf{A}_2\mathbf{h}, \cdots, \mathbf{A}_K\mathbf{h})\,\mathbf{s} + (\mathbf{B}_1\mathbf{h}, \mathbf{B}_2\mathbf{h}, \cdots, \mathbf{B}_K\mathbf{h})\,\mathbf{s}^* = \mathbf{H}_a\mathbf{s} + \mathbf{H}_b\mathbf{s}^* \tag{2.37}$$

Again, if MIMO channel systems are used, the operation above can be done to each column of the channel matrix $\mathbf{H}$, separately. Take the conjugate of (2.36), and align it with the original equation, resulting in the following linear matrix equation.

$$\begin{bmatrix} \mathbf{y} \\ \mathbf{y}^* \end{bmatrix} = \underbrace{\begin{bmatrix} \mathbf{H}_a & \mathbf{H}_b \\ \mathbf{H}_b^* & \mathbf{H}_a^* \end{bmatrix}}_{\boldsymbol{\mathcal{H}}} \begin{bmatrix} \mathbf{s} \\ \mathbf{s}^* \end{bmatrix} + \begin{bmatrix} \boldsymbol{\xi} \\ \boldsymbol{\xi}^* \end{bmatrix} \tag{2.38}$$

With OSTBC, the following three statements are equivalent:

- $\mathbf{X}(\mathbf{s})$ is OSTBC
- $\boldsymbol{\mathcal{H}}^H\boldsymbol{\mathcal{H}} = \|\mathbf{h}\|^2\mathbf{I}_{2K}$ for any $\mathbf{h} \in \mathbb{C}^M$
- $\mathbf{A}_m^H\mathbf{A}_n + \mathbf{B}_n^H\mathbf{B}_m = \delta_{mn}\mathbf{I}_M$
  $\mathbf{A}_m^H\mathbf{B}_n + \mathbf{A}_n^H\mathbf{B}_m = \mathbf{0}$

Therefore, when OSTBC is implemented, the equivalent channel model is unitary up to a scale, the symbols can be optimally detected symbol-by-symbol if the noise is white and full diversity order of M for MISO channels, MN for MIMO channels, can be achieved.

2.3 Relay Channels

2.3.1 Cooperative Relay Channels

MIMO can provide both diversity and multiplexing with the employment of multiple transmitting antennas and multiple receiving antennas. However, due to the limited power and size of some equipments, the deployment of multiple antennas is impractical in some cases. Cooperative communications provide a solution for those equipments with single antenna by building a virtual antenna array, whose antennas come from different equipments nearby. By sharing the antennas of other devices, the single antenna equipment can have higher transmission rate, better reliability and larger coverage [3, 4, 5, 6, 7, 8, 9, 10, 11]. Cooperative communications take the advantage of virtual antenna array and improve the spectral efficiency, throughput and capacity.

The cooperative communication is based on the relay channels, which was first proposed by [2]. The simple typical relay channel consists of three nodes: one source

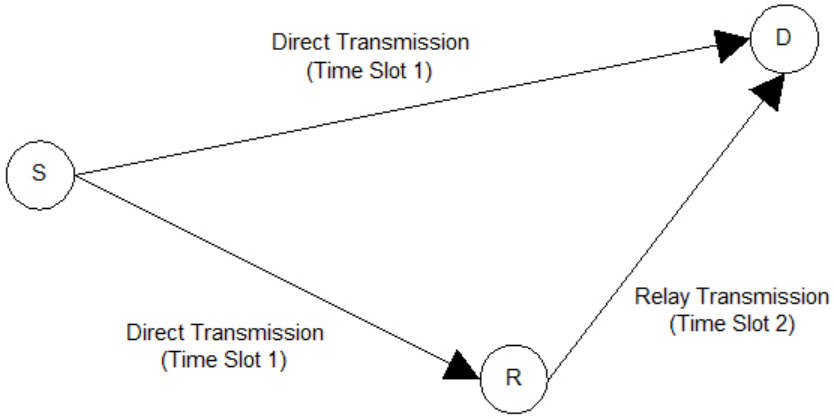

Figure 2.2: Three-Node Relay Channel Model

node, one relay node and one destination node. The system model is illustrated in Figure 2.2. The channel uses two time slots to finish the whole transmission process. In the first time slot, the source node broadcasts the signal to both the destination node and the destination node. In the second phase, the relay node transmits the signals received in the first time slot to the destination node. The destination node will combine the two copies of signals for detection. From the point of source node, it forms a broadcast channel by transmitting to the destination node and relay node. From the point of destination node, the system forms a multiple access channel since the destination node receives the signals from both source node and relay node.

2.3.2 Distributed Relay Channels

Cooperative relay channels are practical in many cases and have been studied thoroughly in the past several decades. When the direct link between the source node and destination node is not feasible, the transmission only relys on the relay nodes between the source node and destination node. The system model can be described with Figure 2.3. There are N relay nodes distributed between the source node and

destination node and there is no direct link between the source node and destination node. The nodes may have single or multiple antennas. The system uses two phases to complete a whole transmission. In the first phase, the source node broadcasts the signals to all of the relay nodes, simultaneously, forming a broadcast channel. At the relay nodes, some processing techniques may be employed. In the second phase, all of the N relay nodes will forward the processed signals to the destination node, simultaneously, forming a multiple access channel. This channel model has received much attention in the past several years[7, 9, 12, 18, 19]. Jing-Hassibi studied this model in detail in [12], showing that the PEP behaves as $(\log P/P)^{\min\{T,N\}}$, with T the coherence internal, N the number of relay nodes and P the total transmit power. The system has the same diversity order as a multiple antenna system, apart from the factor $\log P$, which is due to the product of channel coefficients in two phases. The factor $\log P$ can be ignored when the SNR is sufficiently high, achieving the asymptotic full diversity order. The authors also show that at low and high SNR, the coding gain is the same as that of a multiple antenna channel with N antennas. When the SNR is intermediate, the design of STBC can affect the coding gain considerably.

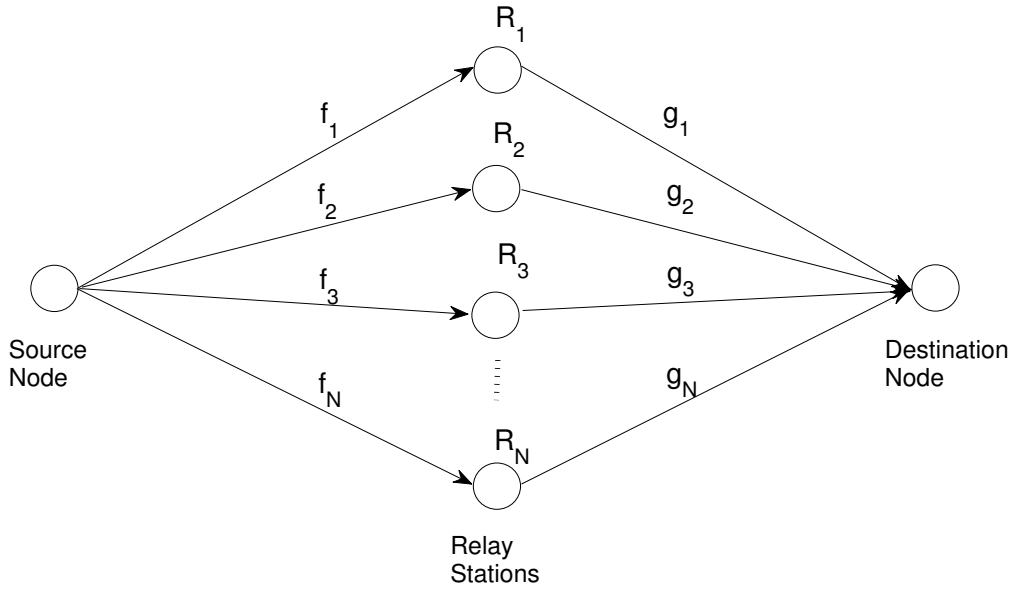

Figure 2.3: System model of single antenna distributed relay channels

Chapter 3

Orthogonally-Distributed Space-Time Codes (ODSTBC) for Single Antenna Distributed Relay Channels

When the OSTBC is directly applied to the single antenna distributed relay channels, the orthogonal condition for the equivalent channel matrix $\boldsymbol{\mathcal{H}}^H\boldsymbol{\mathcal{H}} = \|\mathbf{h}\|^2\mathbf{I}_{2K}$ cannot be achieved due to the two-phase transmission. In this chapter, a new design that could make the equivalent channel matrix be *Orthogonally Distributed* (OD) for a suboptimal symbol-by-symbol detector (SBSD) is proposed. With this design, an asymptotic symbol error probability (SEP) formula with SBSD is derived, showing the optimal diversity function $\frac{\ln^N \rho}{\rho^N}$ is achieved. In addition, two kind of ODSTBC designs for the distributed relay networks are presented, which interestingly renders

that SBSD is equivalent to the ML detector. When the SBSD is implemented, the computation simplicity and optimal diversity function could be achieved simultaneously.

3.1 Channel Model

The distributed cooperative relay networks system model is depicted in Figure 2.3. The system is deployed with $N+2$ nodes: One source node, one destination node and N relay nodes, each being equipped with single antenna. In a whole two-phase transmission process, K symbols are transmitted from the source node to the destination node. In this channel model, we assume that the transmission process is finished in two phases, the first of which has K time slots while the second one has $L \geq K$ slots. In the first K time slots, K symbols are broadcasted consecutively from the source node to the relay stations, simultaneously. A linear dispersion coding scheme is then adopted at the relay nodes. In the second phase, each relay node transmits the processed signals to the destination node in L consecutive time slots, simultaneously. As is commonly known, the (relative) symbol rate of this system is defined as the number of symbol transmitted per time slot utilized in the second phase, i.e. K/L. The channel coefficient between the nth relay and the source node is denoted as f_n, while the channel coefficient between the nth relay and destination node is $g_n, n = 1, \cdots N$. All of these coefficients are assumed to be independent and identically distributed (*i.i.d.*) zero-mean circular symmetric complex Gaussian random variables with unit variance. Besides, the channels are assumed to be quasi-static and flat fading. The channel coefficients remain the same in a two-phase transmission process and change

randomly to other values in another two-phase transmission process. The final detection at the destination node is to combine all the receiving signals from N relays. For practical purposes, we assume that the relay stations don't have channel state information (CSI) in two phases, while the destination node can have full CSI from source to relay and from relay to destination through training sequences. Since the relays are distributed in different locations, we also assume that individual linear processing is performed at each relay station and there's no collaboration between relay stations.

In the first phase, the signal received at the nth relay is

$$\mathbf{r}_n = f_n \mathbf{x} + \mathbf{n}_n, \tag{3.1}$$

where $\mathbf{r}_n = [r_{n1}, r_{n2}, \cdots, r_{nK}]^T$, $\mathbf{x} = [x_1, x_2, \cdots, x_K]^T$ and $\mathbf{n}_n = [n_{n1}, n_{n2}, \cdots, n_{nK}]^T$. The transmitted symbols are assumed to be randomly picked up from a quantized M-ary square QAM modulation with $\mathbb{E}[xx^*] = 1$. The noise vectors are assumed to be zero-mean circular symmetric complex Gaussian white noise with covariance matrix $\mathbb{E}[\mathbf{n}_k \mathbf{n}_l^H] = \delta_{kl}\sigma^2 \mathbf{I}_K$, where $\delta_{kl} = \begin{cases} 1, & k = l \\ 0, & k \neq l \end{cases}$. Then, a Linear Dispersion coding scheme is adopted at the relay nodes, i.e. the signal retransmitted at the nth relay is a linear combination of the received symbol vector and its conjugate version:

$$\mathbf{z}_n = \mathbf{A}_n \mathbf{r}_n + \mathbf{B}_n \mathbf{r}_n^*, \tag{3.2}$$

where $\mathbf{A}_n \in \mathbb{C}^{L \times K}$ and $\mathbf{B}_n \in \mathbb{C}^{L \times K}, n = 1, 2, \cdots, N$.

In the second phase of L consecutive time slots, each relay node forwards these

coded signals to the destination node, simultaneously. The signal vector received at the destination is

$$\begin{aligned}\mathbf{y} &= [\mathbf{z}_1, \mathbf{z}_2, \cdots, \mathbf{z}_N]\mathbf{g} + \mathbf{v} \\ &= [f_1\mathbf{A}_1\mathbf{x}, \cdots, f_N\mathbf{A}_N\mathbf{x}]\mathbf{g} + [f_1^*\mathbf{B}_1\mathbf{x}^*, \cdots, f_N^*\mathbf{B}_N\mathbf{x}^*]\mathbf{g} \\ &+ [\mathbf{A}_1\mathbf{n}_1 + \mathbf{B}_1\mathbf{n}_1^*, \cdots, \mathbf{A}_N\mathbf{n}_N + \mathbf{B}_N\mathbf{n}_N^*]\mathbf{g} + \mathbf{v},\end{aligned} \tag{3.3}$$

where the noise at the destination node $\mathbf{v}$ is also assumed to be zero-mean circular symmetric complex Gaussian white noise with covariance matrix $\mathbb{E}[\mathbf{v}\mathbf{v}^H] = \sigma^2\mathbf{I}_L$ and the channel vector in the second phase is $\mathbf{g}^T = [g_1, g_2, \cdots, g_N]$. In this Amplify-and-Forward (AF) relay system, the noise at the relay nodes is also linearly processed and transmitted to the destination node. The overall noise received at the destination node is

$$\boldsymbol{\eta} = [\mathbf{A}_1\mathbf{n}_1 + \mathbf{B}_1\mathbf{n}_1^*, \cdots, \mathbf{A}_N\mathbf{n}_N + \mathbf{B}_N\mathbf{n}_N^*]\mathbf{g} + \mathbf{v} \tag{3.4}$$

The covariance matrix of noise at the destination node is

$$\mathbf{R} = \mathrm{E}[\boldsymbol{\eta}\boldsymbol{\eta}^H] = \sigma^2\left[\mathbf{I}_L + \sum_{n=1}^{N}|g_n|^2(\mathbf{A}_n\mathbf{A}_n^H + \mathbf{B}_n\mathbf{B}_n^H)\right] \tag{3.5}$$

As described by the expression of noise covariance matrix above, the covariance matrix is related to the linear processing matrices at the relay stations. The unitary structure of noise covariance matrix is desired for simplified detection. However, since $\mathbf{A}_n \in \mathbb{C}^{L\times K}$ and $\mathbf{B}_n \in \mathbb{C}^{L\times K}$ are tall matrices, the identity covariance matrix of the overall noise cannot be achieved.

With some trivial matrix manipulations, the signal model (3.3) could be rewritten

in the following compact form.

$$\mathbf{y} = \boldsymbol{\mathcal{A}}\mathbf{x} + \boldsymbol{\mathcal{B}}\mathbf{x}^* + \boldsymbol{\eta} \tag{3.6}$$

where $\boldsymbol{\mathcal{A}} = \sum_{n=1}^{N} h_n \mathbf{A}_n$, $\boldsymbol{\mathcal{B}} = \sum_{n=1}^{N} \bar{h}_n \mathbf{B}_n$, $h_n = f_n g_n$ and $\bar{h}_n = f_n^* g_n$.

For Maximum Likelihood (ML) detection, it's to solve the following optimization problem

$$\arg\min_{\hat{\mathbf{x}}} \left(\boldsymbol{\mathcal{A}}\hat{\mathbf{x}} + \boldsymbol{\mathcal{B}}\hat{\mathbf{x}}^* - \mathbf{y}\right)^H \mathbf{R}^{-1} \left(\boldsymbol{\mathcal{A}}\hat{\mathbf{x}} + \boldsymbol{\mathcal{B}}\hat{\mathbf{x}}^* - \mathbf{y}\right) \tag{3.7}$$

The computation complexity grows exponentially as the number of symbols transmitted. The structure above is not easy to simplify with existing algorithms or Orthogonal Space-Time Block Code. In some literatures, such as [18, 19], etc., Single Symbol Decodable structures are imposed by expanding $(\boldsymbol{\mathcal{A}}\hat{\mathbf{x}} + \boldsymbol{\mathcal{B}}\hat{\mathbf{x}}^* - \mathbf{y})^H \mathbf{R}^{-1} (\boldsymbol{\mathcal{A}}\hat{\mathbf{x}} + \boldsymbol{\mathcal{B}}\hat{\mathbf{x}}^* - \mathbf{y})$ into a series of matrices, each entry of which only depends on one transmitted symbol $x_k, k = 1, 2, \cdots, K$. In this chapter, a family of Orthogonally Distributed code structures are proposed by verifying the orthogonal conditions of equivalent channel model.

3.2 Orthogonal Design Criteria

In order to manipulate of the equivalent channel model, we take the conjugate of the equation (3.6) and stack the two equations in the following form:

$$\begin{bmatrix} \mathbf{y} \\ \mathbf{y}^* \end{bmatrix} = \begin{bmatrix} \boldsymbol{\mathcal{A}} & \boldsymbol{\mathcal{B}} \\ \boldsymbol{\mathcal{B}}^* & \boldsymbol{\mathcal{A}}^* \end{bmatrix} \begin{bmatrix} \mathbf{x} \\ \mathbf{x}^* \end{bmatrix} + \begin{bmatrix} \boldsymbol{\eta} \\ \boldsymbol{\eta}^* \end{bmatrix}. \tag{3.8}$$

The structure above is very similar to that of OSTBC in MISO systems in (2.38). We introduce the orthogonal conditions for ODSTBC here and define the effective channel matrix in the equation above as

$$\boldsymbol{\mathcal{H}} = \begin{bmatrix} \boldsymbol{\mathcal{A}} & \boldsymbol{\mathcal{B}} \\ \boldsymbol{\mathcal{B}}^* & \boldsymbol{\mathcal{A}}^* \end{bmatrix}. \tag{3.9}$$

Definition 1. *It is said that* $\{\mathbf{A}_n, \mathbf{B}_n\}_{n=1}^N$ *is orthogonally distributed (OD) if*

$$\boldsymbol{\mathcal{H}}^H \boldsymbol{\mathcal{H}} = \|\mathbf{h}\|^2 \mathbf{I}. \tag{3.10}$$

for any complex numbers f_n *and* $g_n,\ n = 1, 2, \ldots, N$.

With the definition above, we have the following theorem with regard to the orthogonality of the equivalent channel matrix $\boldsymbol{\mathcal{H}}$.

Theorem 1. $\{\mathbf{A}_n, \mathbf{B}_n\}_{n=1}^N$ *is orthogonally distributed if and only if the following three conditions are satisfied simultaneously:*

- $\mathbf{A}_n^H \mathbf{A}_n + \mathbf{B}_n^T \mathbf{B}_n^* = \mathbf{I}$
- $\mathbf{A}_m^H \mathbf{A}_n = \mathbf{0},\ \mathbf{B}_m^H \mathbf{B}_n = \mathbf{0}$ *for* $m \neq n$
- $\mathbf{A}_m^H \mathbf{B}_n + \mathbf{B}_n^T \mathbf{A}_m^* = \mathbf{0}$

Proof. In order to have easier deriving process, we exchange the columns of linear processing matrices and thus create a new series of matrices $\bar{\mathbf{A}}_k \in \mathbb{C}^{L \times L}, k = 1, 2, \cdots, K$ and $\bar{\mathbf{B}}_k \in \mathbb{C}^{L \times L}, k = 1, 2, \cdots, K$. Therefore, the effective channel model can be rewritten as

$$\boldsymbol{\mathcal{A}} = \sum_{n=1}^{N} h_n \mathbf{A}_n = [\bar{\mathbf{A}}_1 \mathbf{h}, \bar{\mathbf{A}}_2 \mathbf{h}, \cdots, \bar{\mathbf{A}}_K \mathbf{h}] \tag{3.11}$$

$$\boldsymbol{\mathcal{B}} = \sum_{n=1}^{N} \bar{h}_n \mathbf{B}_n = [\bar{\mathbf{B}}_1 \bar{\mathbf{h}}, \bar{\mathbf{B}}_2 \bar{\mathbf{h}}, \cdots, \bar{\mathbf{B}}_K \bar{\mathbf{h}}], \tag{3.12}$$

where the kth column of $\bar{\mathbf{A}}_l$ and $\bar{\mathbf{B}}_l$ is the lth column of $\mathbf{A}_k$ and $\mathbf{B}_k$, respectively. The equivalent orthogonal conditions with respect to $\bar{\mathbf{A}}_k$ and $\bar{\mathbf{B}}_k$ can be easily calculated:

- $\bar{\mathbf{A}}_k^H \bar{\mathbf{A}}_l + \bar{\mathbf{B}}_l^H \bar{\mathbf{B}}_k = \delta_{kl} \mathbf{I}$
- $[\bar{\mathbf{A}}_k^H \bar{\mathbf{A}}_l]_{ij} = 0$, $[\bar{\mathbf{B}}_l^H \bar{\mathbf{B}}_k]_{ij} = 0$ for all $i \neq j$
- $\bar{\mathbf{A}}_k^H \bar{\mathbf{B}}_l + \bar{\mathbf{A}}_l^H \bar{\mathbf{B}}_k = \mathbf{0}$

Then, the proof process is to prove the equivalent orthogonal conditions for $\bar{\mathbf{A}}_k$ and $\bar{\mathbf{B}}_k$, which is completed in two parts:

1) f_i is real for all $1 \leq i \leq N$;

2) f_i is complex for all $1 \leq i \leq N$.

1) The first part is trivial due to its similarity to the structure of Orthogonal Space Time Block Code. When f_i is real, we can easily verify that the conditions for (3.10) is

$$\bar{\mathbf{A}}_k^H \bar{\mathbf{A}}_l + \bar{\mathbf{B}}_l^H \bar{\mathbf{B}}_k = \delta_{kl} \mathbf{I} \tag{3.13}$$

$$\bar{\mathbf{A}}_k^H \bar{\mathbf{B}}_l + \bar{\mathbf{A}}_l^H \bar{\mathbf{B}}_k = \mathbf{0}. \tag{3.14}$$

The conditions above are equivalent to the strict orthogonality of OSTBC.

2) When f_i is complex for all $1 \leq i \leq N$, we have to treat $\mathbf{h}$ and $\bar{\mathbf{h}}$ differently. We denote the diagonal matrix of f_i as $\mathbf{D} = \text{diag}(f_1, f_2, \cdots, f_N)$. Therefore,

$$\boldsymbol{\mathcal{A}} = [\bar{\mathbf{A}}_1 \mathbf{h}, \bar{\mathbf{A}}_2 \mathbf{h}, \cdots, \bar{\mathbf{A}}_K \mathbf{h}] = [\tilde{\mathbf{A}}_1 \mathbf{g}, \tilde{\mathbf{A}}_2 \mathbf{g}, \cdots, \tilde{\mathbf{A}}_K \mathbf{g}] \tag{3.15}$$

$$\boldsymbol{\mathcal{B}} = [\bar{\mathbf{B}}_1\bar{\mathbf{h}}, \bar{\mathbf{B}}_2\bar{\mathbf{h}}, \cdots, \bar{\mathbf{B}}_K\bar{\mathbf{h}}] = [\tilde{\mathbf{B}}_1\mathbf{g}, \tilde{\mathbf{B}}_2\mathbf{g}, \cdots, \tilde{\mathbf{B}}_K\mathbf{g}], \tag{3.16}$$

where $\tilde{\mathbf{A}}_k = \bar{\mathbf{A}}_k\mathbf{D}$ and $\tilde{\mathbf{B}}_k = \bar{\mathbf{B}}_k\mathbf{D}^*$. Substituting (3.15) and (3.16) into the orthogonal constraint (3.10), we could get the following two equations after some straightforward calculation steps.

$$\tilde{\mathbf{A}}_k^H\tilde{\mathbf{A}}_l + \tilde{\mathbf{B}}_l^H\tilde{\mathbf{B}}_k = \delta_{kl}\mathbf{D}\mathbf{D}^* \tag{3.17}$$

$$\tilde{\mathbf{A}}_k^H\tilde{\mathbf{B}}_l + \tilde{\mathbf{A}}_l^H\tilde{\mathbf{B}}_k = \mathbf{0} \tag{3.18}$$

Substituting $\tilde{\mathbf{A}}_k = \bar{\mathbf{A}}_k\mathbf{D}$ and $\tilde{\mathbf{B}}_k = \bar{\mathbf{B}}_k\mathbf{D}^*$ into the equations above

$$\mathbf{D}^H\bar{\mathbf{A}}_k^H\bar{\mathbf{A}}_l\mathbf{D} + \mathbf{D}\bar{\mathbf{B}}_l^H\bar{\mathbf{B}}_k\mathbf{D}^* = \delta_{kl}\mathbf{D}\mathbf{D}^* \tag{3.19}$$

$$\mathbf{D}^H\bar{\mathbf{A}}_k^H\bar{\mathbf{B}}_l\mathbf{D}^* + \mathbf{D}^H\bar{\mathbf{A}}_l^H\bar{\mathbf{B}}_k\mathbf{D}^* = \mathbf{0} \tag{3.20}$$

As with (3.19), the derivation was discussed in two cases: a) $k \neq l$; b) $k = l$.

a) When $k \neq l$, from (3.19),

$$\mathbf{D}^H\bar{\mathbf{A}}_k^H\bar{\mathbf{A}}_l\mathbf{D} + \mathbf{D}\bar{\mathbf{B}}_l^H\bar{\mathbf{B}}_k\mathbf{D}^* = \mathbf{0}. \tag{3.21}$$

If $i = j$, the equation above is

$$|f_i|^2[\bar{\mathbf{A}}_k^H\bar{\mathbf{A}}_l]_{ii} + |f_i|^2[\bar{\mathbf{B}}_l^H\bar{\mathbf{B}}_k]_{ii} = \mathbf{0} \tag{3.22}$$

for all possible values $|f_i|$. Therefore, the equation above holds if and only if $[\bar{\mathbf{A}}_k^H\bar{\mathbf{A}}_l]_{ii} + [\bar{\mathbf{B}}_l^H\bar{\mathbf{B}}_k]_{ii} = 0$. If $i \neq j$, the condition in (3.21) is

$$f_i^*f_j[\bar{\mathbf{A}}_k^H\bar{\mathbf{A}}_l]_{ij} + f_if_j^*[\bar{\mathbf{B}}_l^H\bar{\mathbf{B}}_k]_{ij} = \mathbf{0} \tag{3.23}$$

For all combinations of f_i and f_j, the equation above holds if and only if $[\bar{\mathbf{A}}_k^H \bar{\mathbf{A}}_l]_{ij} = [\bar{\mathbf{B}}_l^H \bar{\mathbf{B}}_k]_{ij} = 0$. Therefore, when $k \neq l$, the sum of diagonal values of $[\bar{\mathbf{A}}_k^H \bar{\mathbf{A}}_l]_{ij}$ and $[\bar{\mathbf{B}}_l^H \bar{\mathbf{B}}_k]_{ij}$ should be zero, while the non-diagonal values of these two matrices are all zero. The first and the second condition in theorem is thus proved.

b) When $k = l$, from (3.19),

$$\mathbf{D}^H \bar{\mathbf{A}}_k^H \bar{\mathbf{A}}_k \mathbf{D} + \mathbf{D} \bar{\mathbf{B}}_k^H \bar{\mathbf{B}}_k \mathbf{D}^* = \mathbf{D}\mathbf{D}^*. \tag{3.24}$$

If $i = j$, the equation above is

$$|f_i|^2 [\bar{\mathbf{A}}_k^H \bar{\mathbf{A}}_k]_{ii} + |f_i|^2 [\bar{\mathbf{B}}_k^H \bar{\mathbf{B}}_k]_{ii} = |f_i|^2, \tag{3.25}$$

which means $[\bar{\mathbf{A}}_k^H \bar{\mathbf{A}}_k]_{ii} + [\bar{\mathbf{B}}_k^H \bar{\mathbf{B}}_k]_{ii} = 1$ for all possible values of f_i. If $i \neq j$, the condition is the same as (3.23), which means $[\bar{\mathbf{A}}_k^H \bar{\mathbf{A}}_k]_{ij} = [\bar{\mathbf{B}}_k^H \bar{\mathbf{B}}_k]_{ij} = 0$ for all possible values of f_i and f_j.

Therefore, the condition (3.19) holds if and only if the sum of diagonal values of $\bar{\mathbf{A}}_k^H \bar{\mathbf{A}}_l$ and $\bar{\mathbf{B}}_l^H \bar{\mathbf{B}}_k$ is 0 (when $k \neq l$) or 1 (when $k = l$), while the non-diagonal values of these matrices are all zero. Now we have proved the first and the second condition in the theorem.

If we reformulate (3.20) in the same procedure, we can easily prove the third condition in the theorem by verifying thatf $\bar{\mathbf{A}}_k^H \bar{\mathbf{B}}_l + \bar{\mathbf{A}}_l^H \bar{\mathbf{B}}_k = 0$, whether $k = l$ or not.

Since the proof process is equivalently reversible, the conditions we proposed are equivalent to the strict orthogonal constraint. Hence, the theorem is proved. □

3.3 Diversity Function Analysis

As is illustrated in the previous section, when the conditions in Theorem 1 are satisfied simultaneously, the equivalent channel matrix $\boldsymbol{\mathcal{H}}$ is unitary up to a scale, i.e. $\boldsymbol{\mathcal{H}}^H\boldsymbol{\mathcal{H}} = \|\mathbf{h}\|^2\mathbf{I}$. For ODSTBC, multiplying (3.8) with $\boldsymbol{\mathcal{H}}^H$ and taking the first half of the signal vector yield

$$\tilde{\mathbf{y}} = \|\mathbf{h}\|^2\mathbf{x} + \tilde{\boldsymbol{\eta}}, \tag{3.26}$$

where $\tilde{\boldsymbol{\eta}} = \boldsymbol{\mathcal{A}}^H\boldsymbol{\eta} + \boldsymbol{\mathcal{B}}^T\boldsymbol{\eta}^*$. This leads to the following suboptimal SBSD:

$$\hat{\mathbf{x}} = \arg\min_{\mathbf{x}} \left\|\tilde{\mathbf{y}} - \|\mathbf{h}\|^2\mathbf{x}\right\|. \tag{3.27}$$

Please not that the SBSD is suboptimal when the covariance matrix of $\tilde{\boldsymbol{\eta}}$ is not identity matrix up to a scale. Particularly, when the covariance matrix of $\tilde{\boldsymbol{\eta}}$, $\tilde{\mathbf{R}} = \mathbb{E}[\tilde{\boldsymbol{\eta}}\tilde{\boldsymbol{\eta}}^H]$, is an identity matrix up to a scale, the SBSD is equivalent to the ML detector. Now, let us analyze the error performance of the SBSD (3.27). The SEP performance of SBSD could be described with the following theorem.

Theorem 2. $\bar{\mathrm{P}}_{SEP}$*, the average SEP with M-ary square QAM, of SBSD for the channel* (3.26) *can be represented by*

$$\bar{\mathrm{P}}_{SEP} = \phi(M,N)\left(\ln\rho/\rho\right)^N + \mathcal{O}((\ln\rho)^{N-1}/\rho^N),$$

where $\phi(M,N) = \frac{2^{N+2}(M-1)^N}{3^N\pi}\left(1-\frac{1}{\sqrt{M}}\right)\left[\int_{\frac{\pi}{4}}^{\frac{\pi}{2}}\sin^{2N}\theta\mathrm{d}\theta + \frac{1}{\sqrt{M}}\int_0^{\frac{\pi}{4}}\sin^{2N}\theta\mathrm{d}\theta\right]$*, when* SNR *is sufficiently large. Therefore, the SBSD could achieve asymptotic full diversity with square QAM constellation.*

Proof. See Appendix A.1. □

3.4 Orthogonal Design Method

Due to the strict orthogonal conditions introduced in the previous section, as the number of relays increases, the symbol rate is expected to decrease. In this Section, we discuss the scenario of transmitting $K < L$ symbols, i.e. rate $K/L < 1$, in a two-phase transmission.

We refer to the original covariance matrix expression in (3.5) again to discuss the structure of noise. From (3.5), the noise covariance matrix is

$$\mathbf{R} = \sigma^2 \left[\mathbf{I} + \sum_{n=1}^{N} |g_n|^2 (\mathbf{A}_n \mathbf{A}_n^H + \mathbf{B}_n \mathbf{B}_n^H) \right]. \tag{3.28}$$

Since $\mathbf{A}_n \in \mathbb{C}^{L\times K}$ and $\mathbf{B}_n \in \mathbb{C}^{L\times K}$ are tall matrices, the noise covariance matrix is not an identity matrix up to a scale. However, we could design linear processing matrices $\mathbf{A}_n \in \mathbb{C}^{L\times K}$ and $\mathbf{B}_n \in \mathbb{C}^{L\times K}$ such that the noise covariance matrix for SBSD detection $\tilde{\mathbf{R}} = \mathbb{E}[\tilde{\boldsymbol{\eta}}\tilde{\boldsymbol{\eta}}^H] = \mathbb{E}[(\boldsymbol{\mathcal{A}}^H\boldsymbol{\eta} + \boldsymbol{\mathcal{B}}^T\boldsymbol{\eta}^*)(\boldsymbol{\mathcal{A}}^H\boldsymbol{\eta} + \boldsymbol{\mathcal{B}}^T\boldsymbol{\eta}^*)^H]$ is an identity matrix up to a scale. If $\tilde{\mathbf{R}}$ is an identity matrix up to a scale, the SBSD will be equivalent to the ML detector.

In this section, a simple design for ODSTBC are proposed, which make the SBSD equivalent to the ML detector. If we denote the code structure by $\mathcal{X}(f_i, \mathbf{s}) = [f_1\mathbf{A}_1\mathbf{x} + f_1^*\mathbf{B}_1\mathbf{x}^*, \cdots, f_N\mathbf{A}_N\mathbf{x} + f_N^*\mathbf{B}_N\mathbf{x}^*]$ and use $\mathcal{X}(\mathbf{s}) = [\mathbf{A}_1\mathbf{x} + \mathbf{B}_1\mathbf{x}^*, \cdots, \mathbf{A}_N\mathbf{x} + \mathbf{B}_N\mathbf{x}^*]$ to illustrate orthogonality for simplicity, two simple designs based on the Alamouti coding scheme to construct Rate-$2/2^n$ ODSTBC is shown below. The rate of $2/2^n$ means transmitting 2 symbols with 2^n time slots utilized in the second phase. Therefore, the code is especially designed for the scenario where the number of relays deployed is the power of 2.

Design 1. *Any even number of symbols can be transmitted simultaneously in one transmission with the following structure.*

$$\mathcal{X}(\mathbf{s}) = \left(\otimes^{n-1}\mathbf{I}\right) \otimes \left\{ \mathbf{e}_1 \otimes \begin{bmatrix} x_1 & -x_2^* \\ x_2 & x_1^* \end{bmatrix} + \mathbf{e}_2 \otimes \begin{bmatrix} x_3 & -x_4^* \\ x_4 & x_3^* \end{bmatrix} + \cdots \right\},$$

where $\mathbf{e}_i = [0, \ldots, 0, 1, 0, \ldots, 0]^T$.

The symbol rate for Design 1 is $\mathcal{R} = 2^{1-n}$ per channel slot use in the second phase, where 2^n is also the number of antennas employed. By substituting the orthogonal conditions in Theorem 1 into the calculation of $\tilde{\mathbf{R}}$ and allowing either $\mathbf{A}_i$ or $\mathbf{B}_i$ is zero, the structure of linear processing matrices produces $\mathcal{A} = \left[\begin{smallmatrix} 1 & 1 & 1 & 1 & \cdots & 1 & 1 \end{smallmatrix}\right]^T$ and $\mathcal{B} = \left[\begin{smallmatrix} -1 & 1 & -1 & 1 & \cdots & -1 & 1 \end{smallmatrix}\right]^T$. We can easily verify that the covariance matrix is an identity matrix up to a scale in that $\mathcal{A}$ and $\mathcal{B}$ sum up the diagonal values in $\mathbf{R}$. One of the significant advantages of these two ODSTBC designs is that the noise covariance matrix $\tilde{\mathbf{R}}$ in (3.26) is an identity matrix up to a scale, which makes SBSD equivalent to the ML detector. This is the major difference between the OSTBC designs presented in this paper and the designs proposed in [18]. The following is a specific example to demonstrate this difference.

Example 1. *Consider a specific rate-2/4 ODSTBC for a cooperative network with four relays using Design 1, where*

$$\mathcal{X}(\mathbf{s}) = \mathrm{diag}\left\{ \begin{bmatrix} x_1 & -x_2^* \\ x_2 & x_1^* \end{bmatrix}, \begin{bmatrix} x_1 & -x_2^* \\ x_2 & x_1^* \end{bmatrix} \right\}.$$

The mapping matrices $\mathbf{A}_n \in \mathbb{C}^{L\times K}$ *and* $\mathbf{B}_n \in \mathbb{C}^{L\times K}$ *can be chosen according to the*

conditions in Theorem 1, as follows:

$$\mathbf{A}_1 = \begin{bmatrix} 1 & 0 \\ 0 & 1 \\ 0 & 0 \\ 0 & 0 \end{bmatrix}, \quad \mathbf{A}_3 = \begin{bmatrix} 0 & 0 \\ 0 & 0 \\ 1 & 0 \\ 0 & 1 \end{bmatrix}, \quad \mathbf{B}_2 = \begin{bmatrix} 0 & -1 \\ 1 & 0 \\ 0 & 0 \\ 0 & 0 \end{bmatrix}, \quad \mathbf{B}_4 = \begin{bmatrix} 0 & 0 \\ 0 & 0 \\ 0 & -1 \\ 1 & 0 \end{bmatrix}, \tag{3.29}$$

and $\mathbf{A}_2 = \mathbf{A}_4 = \mathbf{B}_1 = \mathbf{B}_3 = \mathbf{0}$. *Changing the columns of* $\mathbf{A}_k$ *and* $\mathbf{B}_k$, *the precoding matrices become*

$$\bar{\mathbf{A}}_1 = \begin{bmatrix} 1 & 0 & 0 & 0 \\ 0 & 0 & 0 & 0 \\ 0 & 0 & 1 & 0 \\ 0 & 0 & 0 & 0 \end{bmatrix}, \bar{\mathbf{A}}_2 = \begin{bmatrix} 0 & 0 & 0 & 0 \\ 1 & 0 & 0 & 0 \\ 0 & 0 & 0 & 0 \\ 0 & 0 & 1 & 0 \end{bmatrix}, \bar{\mathbf{B}}_1 = \begin{bmatrix} 0 & 0 & 0 & 0 \\ 0 & 1 & 0 & 0 \\ 0 & 0 & 0 & 0 \\ 0 & 0 & 0 & 1 \end{bmatrix}, \bar{\mathbf{B}}_2 = \begin{bmatrix} 0 & -1 & 0 & 0 \\ 0 & 0 & 0 & 0 \\ 0 & 0 & 0 & -1 \\ 0 & 0 & 0 & 0 \end{bmatrix}. \tag{3.30}$$

Substituting the mapping matrices in (3.5) *, the covariance matrix of the noise* $\boldsymbol{\eta}$ *in* (3.6) *is* $\mathbf{R} = \sigma^2 \text{diag}\{1+|g_1|^2+|g_2|^2, 1+|g_1|^2+|g_2|^2, 1+|g_3|^2+|g_4|^2, 1+|g_3|^2+|g_4|^2\}$, *which is a diagonal matrix. However the diagonal values are not exactly equal. The covariance matrix of the noise* $\tilde{\boldsymbol{\eta}}$ *in* (3.26) *is an identity matrix up to a scale. In fact, by subsitutiting the mapping matrices into* $\tilde{\mathbf{R}} = \mathbb{E}[\tilde{\boldsymbol{\eta}}\tilde{\boldsymbol{\eta}}^H]$, $\tilde{\mathbf{R}} = \sigma^2(\|\mathbf{h}\|^2 + (|g_1|^2 + |g_2|^2)(|h_1|^2 + |h_2|^2) + (|g_3|^2 + |g_4|^2)(|h_3|^2 + |h_4|^2))\mathbf{I}$. *Therefore, with the structures proposed in Design 1, the suboptimal detection method SBSD is actually equivalent to the ML detection.*

Chapter 4

Alamouti Based Toeplitz Space-Time Block Codes (ABTSTBC) for Two-antenna Distributed Relay Channels

The ODSTBC proposed in the former chapter could achieve both asymptotic full diversity and low computational complexity with symbol-by-symbol detection. The code structure is favorable in single antenna distributed relay channels when the number of relays is small. However, if more and more relays are deployed, the symbol rate will decrease dramatically, as shown by the symbol rate $\mathcal{R} = 2^{1-n}$. In order to solve this problem, a nonorthogonal code structure by relieving the restrictive orthogonal conditions is proposed in this chapter and a two-antenna distributed relay channel

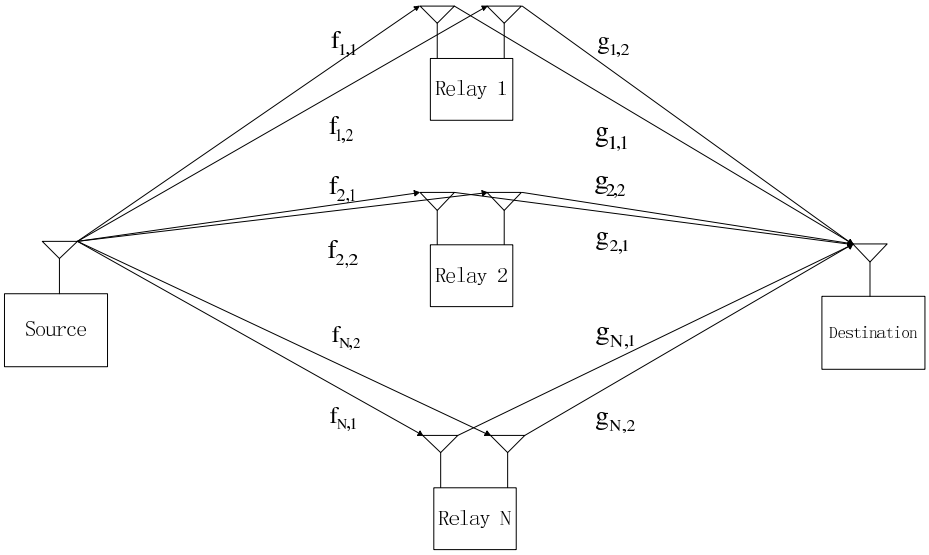

Figure 4.1: System model of two-antenna distributed relay channels

model is utilized. In this chapter, an Alamouti Based Toeplitz STBC structure is proposed, which has block Toeplitz structures in both the code matrix and the equivalent channel matrix. With the linear suboptimal symbol-by-symbol detector (SBSD), the code can achieve the optimal diversity function of $\frac{\ln^N \rho}{\rho^{2N}}$, where N is the number of relay nodes.

4.1 Two-Antenna Relay Channel Model

The distributed cooperative relay networks system model is depicted in the Figure 4.1. The system is also deployed with $N+2$ nodes: One source node, one destination node and N relay nodes. The source node and destination node are equipped with single antenna while all of the relay nodes are equipped with two antennas. In a whole two-phase transmission process, K symbols are transmitted from the source node to the destination node. In this channel model, we assume that the transmission process

is completed in two phases, the first of which has K time slots while the second one has $L > K$ slots. In the first K time slots, K symbols are broadcasted consecutively from the source node to the N relay nodes. A linear dispersion coding scheme is then adopted at the relay nodes bofore each of the L slots. In the second phase, each relay node transmits the processed signals to the destination node in L consecutively time slots, simultaneously. As is introduced in the former chapter, the (relative) symbol rate of this system is defined as K/L [12]. The channel vector between the jth relay and the source node is denoted as $\mathbf{f}_j = [f_{j1}, f_{j2}]^T$, while the channel vector between the jth relay and destination node is $\mathbf{g}_j^T = [g_{j1}, g_{j2}]$. All of these coefficients are assumed to be independent and identically distributed (*i.i.d.*) zero-mean circular symmetric complex Gaussian random variables with unit variance. In addition, the channels are assumed to be quasi-static and flat fading. The channel coefficients remain unchanged in a whole two-phase transmission process and change randomly to other values in the next process. The final detection process at the destination node is to make decisions by combining all received signals from N relays. For practical purposes, we assume that the relay nodes do not have channel state information (CSI), while the destination node can have full CSI from source to relay and from relay to destination through training sequences. In fact, if relay nodes have CSI of the first phase, we may design code structures according to the channel realizations to achieve a better performance. However, in such cases, the code structures will depend on the realization of the channel coefficients and the mapping matrices will have to be updated in every transmission process, which is burdensome when the relay nodes have limited computation abilities or the time delay is critical. For simplicity, we assume that there's no CSI utilized at the relay nodes. Therefore, designing the

mapping structures is independent of the channel realizations. Since the relays are distributed in different locations, we also assume that individual linear processing is performed at each relay node and there's no collaboration between relay nodes.

In the first phase, K time slots are used to transmit K symbols. The transmitted vector is $\mathbf{x} = [x_1, x_2, \cdots, x_K]^T$, whose entries are randomly from a quantized M-ary square QAM constellation, i.e. $\mathbb{E}[\mathbf{x}\mathbf{x}^H] = \mathbf{I}_K$. The signal vector received by the j-th relay node R_j at the k-th time slot can be written as

$$\mathbf{r}_j(k) = \mathbf{f}_j x_k + \mathbf{n}_j(k), \tag{4.1}$$

where $k = 1, \cdots, K$ and $j = 1, 2, \cdots, N$, $\mathbf{r}_j(k) = [r_{j1}(k), r_{j2}(k)]^T$, $\mathbf{f}_j = [f_{j1}, f_{j2}]^T$ and $\mathbf{n}_j(k) = [n_{j1}(k), n_{j2}(k)]^T$. If we stack all K received signal vectors $\mathbf{r}_j(k)$ of the first phase into a $2K \times 1$ vector, i.e. $\mathbf{r}_j = [\mathbf{r}_j(1)^T, \mathbf{r}_j(2)^T \cdots, \mathbf{r}_j(K)^T]^T$, we have the more compact expression of the symbols received at the jth relay node:

$$\mathbf{r}_j = \mathbf{F}_j \mathbf{x} + \mathbf{n}_j, \tag{4.2}$$

where $\mathbf{F}_j = \mathbf{I}_K \otimes \mathbf{f}_j$, $\mathbf{x} = [x_1, x_2, \cdots, x_K]^T$ and $\mathbf{n}_j = [\mathbf{n}_j(1)^T, \mathbf{n}_j(2)^T, \cdots, \mathbf{n}_j(K)^T]^T$.

In the second transmission phase, each relay R_j combines the $2K \times 1$ received signal vector in (4.2) into new symbols using the linear dispersion coding scheme such that

$$\mathbf{z}_j(l) = \mathbf{A}_j(l)\mathbf{r}_j + \mathbf{B}_j(l)\mathbf{r}_j^*, \tag{4.3}$$

where $\mathbf{A}_j(l) \in \mathbb{C}^{2\times 2K}$ and $\mathbf{B}_j(l) \in \mathbb{C}^{2\times 2K}$ are coding matrices for the j-th relay in the l-th time slot of the second phase. The N coded 2×1 vectors of the N relay nodes

$\mathbf{z}_j(l)$ are transmitted to the destination node, simultaneously. Hence, in the l-th time slot, the signal received at destination node can be represented as

$$y_l = \sum_{j=1}^{N} \mathbf{g}_j^T \mathbf{z}_j(l) + \eta_l = \sum_{j=1}^{N} (\mathbf{g}_j^T \mathbf{A}_j(l)\mathbf{r}_j + \mathbf{g}_j^T \mathbf{B}_j(l)\mathbf{r}_j^*) + \eta_l, \tag{4.4}$$

where $\mathbf{g}_j^T = [g_{j1}, g_{j2}]$ is the channel matrix from the jth relay to the destination node. Aligning all the l symbols received in the second phase into a vector $\mathbf{y} = [y_1, y_2, ..., y_L]^T$, we have the following linear matrix equation.

$$\mathbf{y} = \begin{bmatrix} \mathbf{r}_1^T \mathbf{A}_1(1)^T + \mathbf{r}_1^H \mathbf{B}_1(1)^T & \cdots & \mathbf{r}_N^T \mathbf{A}_N(1)^T + \mathbf{r}_N^H \mathbf{B}_N(1)^T \\ \mathbf{r}_1^T \mathbf{A}_1(2)^T + \mathbf{r}_1^H \mathbf{B}_1(2)^T & \cdots & \mathbf{r}_N^T \mathbf{A}_N(2)^T + \mathbf{r}_N^H \mathbf{B}_N(2)^T \\ \vdots & \cdots & \vdots \\ \mathbf{r}_1^T \mathbf{A}_1(L)^T + \mathbf{r}_1^H \mathbf{B}_1(L)^T & \cdots & \mathbf{r}_N^T \mathbf{A}_N(L)^T + \mathbf{r}_N^H \mathbf{B}_N(L)^T \end{bmatrix} \begin{bmatrix} \mathbf{g}_1 \\ \mathbf{g}_2 \\ \vdots \\ \mathbf{g}_N \end{bmatrix} + \boldsymbol{\eta} \tag{4.5}$$

Substituting the vectors $\mathbf{r}_j$ into the equation above, we have the detailed expression of the signal vector at the destination node represented in the following equation.

$$\begin{aligned} \mathbf{y} = & \underbrace{\begin{bmatrix} \mathbf{x}^T \mathbf{F}_1^T \mathbf{A}_1(1)^T + \mathbf{x}^H \mathbf{F}_1^H \mathbf{B}_1(1)^T & \cdots & \mathbf{x}^T \mathbf{F}_N^T \mathbf{A}_N(1)^T + \mathbf{x}^H \mathbf{F}_N^H \mathbf{B}_N(1)^T \\ \mathbf{x}^T \mathbf{F}_1^T \mathbf{A}_1(2)^T + \mathbf{x}^H \mathbf{F}_1^H \mathbf{B}_1(2)^T & \cdots & \mathbf{x}^T \mathbf{F}_N^T \mathbf{A}_N(2)^T + \mathbf{x}^H \mathbf{F}_N^H \mathbf{B}_N(2)^T \\ \vdots & \cdots & \vdots \\ \mathbf{x}^T \mathbf{F}_1^T \mathbf{A}_1(L)^T + \mathbf{x}^H \mathbf{F}_1^H \mathbf{B}_1(L)^T & \cdots & \mathbf{x}^T \mathbf{F}_N^T \mathbf{A}_N(L)^T + \mathbf{x}^H \mathbf{F}_N^H \mathbf{B}_N(L)^T \end{bmatrix}}_{\mathcal{X}(\mathbf{F}_i, \mathbf{x})} \begin{bmatrix} \mathbf{g}_1 \\ \mathbf{g}_2 \\ \vdots \\ \mathbf{g}_N \end{bmatrix} \\ & + \begin{bmatrix} \mathbf{n}_1^T \mathbf{A}_1(1)^T + \mathbf{n}_1^H \mathbf{B}_1(1)^T & \cdots & \mathbf{n}_N^T \mathbf{A}_N(1)^T + \mathbf{n}_N^H \mathbf{B}_N(1)^T \\ \mathbf{n}_1^T \mathbf{A}_1(2)^T + \mathbf{n}_1^H \mathbf{B}_1(2)^T & \cdots & \mathbf{n}_N^T \mathbf{A}_N(2)^T + \mathbf{n}_N^H \mathbf{B}_N(2)^T \\ \vdots & \cdots & \vdots \\ \mathbf{n}_1^T \mathbf{A}_1(L)^T + \mathbf{n}_1^H \mathbf{B}_1(L)^T & \cdots & \mathbf{n}_N^T \mathbf{A}_N(L)^T + \mathbf{n}_N^H \mathbf{B}_N(L)^T \end{bmatrix} \begin{bmatrix} \mathbf{g}_1 \\ \mathbf{g}_2 \\ \vdots \\ \mathbf{g}_N \end{bmatrix} + \boldsymbol{\eta} \end{aligned} \tag{4.6}$$

In order to illustrate the code structure at the relay nodes, we use $\mathcal{X}(\mathbf{F}_i, \mathbf{x})$ to

represent the code structures in (4.6), and use $\mathcal{X}(\mathbf{x})$ to represent the structure, by removing the channel coefficients, for simplicity.

4.2 Design Criteria

In this section, we will discuss the design methods for two-antenna distributed relay channels. Due the fact that all relay nodes are equipped with two antennas, the Space-Time Block Codes designed here are specially used for even number of antennas. In order to make the code structure achieve the optimal diversity function with linear receivers, the Toeplitz structure of STBC in MISO channel is generalized to the distributed two-antenna relay channels. The linear Toeplitz Space-Time Block Code is first proposed by Zhang-Liu-Wong [20]. With the Toeplitz STBC, the authors managed to convert the original MISO flat fading channel into a Toeplitz virtual MIMO channel, which could achieve full diversity with linear receivers. Shang-Xia extended the result of [20] and proposed a series of Overlapped Alamouti Codes in [21], which also achieves full diversity with ZF and MMSE receivers. Based on these results, we generalized the Toeplitz STBC structures in MIMO channels to multiple antenna distributed relay channels. In this thesis, a block Toeplitz code structure, whose blocks are the addition of two alamouti codes, is proposed. With some matrix manipulations, the equivalent channel matrix can also be denoted as a block Toeplitz matrix, whose blocks are the product of two Alamouti structures. The entries of these two matrices come from the two transmission phases, respectively. With this structure and linear SBSD, the code achieves low detection complexity and optimal diversity function.

The code structure proposed is denoted in the following matrix.

$$\mathcal{X}(\mathbf{x}) = \begin{bmatrix} \boldsymbol{\Omega}_{1,2} & & & \\ \boldsymbol{\Omega}_{3,4} & \boldsymbol{\Omega}_{1,2} & & \\ \vdots & \vdots & \ddots & \\ \boldsymbol{\Omega}_{K-1,K} & \boldsymbol{\Omega}_{K-3,K-2} & \cdots & \boldsymbol{\Omega}_{1,2} \\ & \boldsymbol{\Omega}_{K-1,K} & \cdots & \boldsymbol{\Omega}_{3,4} \\ & \ddots & \ddots & \vdots \\ & & \boldsymbol{\Omega}_{K-1,K} & \boldsymbol{\Omega}_{K-3,K-2} \\ & & & \boldsymbol{\Omega}_{K-1,K} \end{bmatrix} \in \mathbb{C}^{(K+2N-2)\times 2N} \tag{4.7}$$

where $\boldsymbol{\Omega}_{k,l} = \begin{bmatrix} x_k + x_l^* & x_k - x_l^* \\ -x_k^* + x_l & x_k^* + x_l \end{bmatrix} = \begin{bmatrix} x_k & -x_l^* \\ x_l & x_k^* \end{bmatrix} + \begin{bmatrix} x_l^* & x_k \\ -x_k^* & x_l \end{bmatrix}$ is the addition of two Alamouti codes and k, l are any positive integers. The mapping matrices $\mathbf{A}_i(l)$ and $\mathbf{B}_i(l)$ are chosen such that each 2×2 block of $\mathcal{X}(\mathbf{F}_i, \mathbf{x})$ has the following structure:

$$\begin{bmatrix} \mathbf{x}^T\mathbf{F}_i^T\mathbf{A}_i(l-1)^T + \mathbf{x}^H\mathbf{F}_i^H\mathbf{B}_i(l-1)^T \\ \mathbf{x}^T\mathbf{F}_i^T\mathbf{A}_i(l)^T + \mathbf{x}^H\mathbf{F}_i^H\mathbf{B}_i(l)^T \end{bmatrix} = \begin{bmatrix} f_{i,1}x_{k-1} + f_{i,2}^*x_k^* & f_{i,2}x_{k-1} - f_{i,1}^*x_k^* \\ -f_{i,2}^*x_{k-1}^* + f_{i,1}x_k & f_{i,1}^*x_{k-1}^* + f_{i,2}x_k \end{bmatrix}, \tag{4.8}$$

where $1 \leq l < L$ is an even integer, k is determined through the block Toeplitz structure of $\mathcal{X}(\mathbf{x})$ and i is the index of relays. Due to the structure of the block Toeplitz matrix, the time slots used in the second phase is $L = K+2N-2$. Therefore, the relative symbol rate is $\frac{K}{K+2N-2}$, which approaches 1 as K increases. The symbol rate will not decrease dramatically as the number of antennas increases, which is the main advantage compared with the code structure proposed in the previous chapter.

Example 2. *When $N = 2$ relays are deployed, the number of antennas is $2N = 4$. We assume there are $K = 4$ symbols transmitted in one transmission process. In*

the second phase, $L = K + 2N - 2 = 6$ *slots are utilized based on the block Toeplitz structure. The specific code structure* $\mathcal{X}(\mathbf{x})$ *is expressed as*

$$\mathcal{X}(\mathbf{x}) = \begin{bmatrix} x_1 + x_2^* & x_1 - x_2^* & & \\ -x_1^* + x_2 & x_1^* + x_2 & & \\ x_3 + x_4^* & x_3 - x_4^* & x_1 + x_2^* & x_1 - x_2^* \\ -x_3^* + x_4 & x_3^* + x_4 & -x_1^* + x_2 & x_1^* + x_2 \\ & & x_3 + x_4^* & x_3 - x_4^* \\ & & -x_3^* + x_4 & x_3^* + x_4 \end{bmatrix} \tag{4.9}$$

The mapping matrices $\mathbf{A}_i(l)$ *and* $\mathbf{B}_i(l)$ *and detailed code structure with channel coefficients can be derived from (4.7) and (4.8). The mapping matrices* $\mathbf{A}_i(l)$ *and* $\mathbf{B}_i(l)$ *are* 2×8 *matrices:*

$$\mathbf{A}_1(1) = \begin{bmatrix} 1 & 0 & 0 & 0 & 0 & 0 & 0 & 0 \\ 0 & 1 & 0 & 0 & 0 & 0 & 0 & 0 \end{bmatrix} \qquad \mathbf{B}_1(1) = \begin{bmatrix} 0 & 0 & 0 & 1 & 0 & 0 & 0 & 0 \\ 0 & 0 & -1 & 0 & 0 & 0 & 0 & 0 \end{bmatrix}$$

$$\mathbf{A}_1(2) = \begin{bmatrix} 0 & 0 & 1 & 0 & 0 & 0 & 0 & 0 \\ 0 & 0 & 0 & 1 & 0 & 0 & 0 & 0 \end{bmatrix} \qquad \mathbf{B}_1(2) = \begin{bmatrix} 0 & -1 & 0 & 0 & 0 & 0 & 0 & 0 \\ 1 & 0 & 0 & 0 & 0 & 0 & 0 & 0 \end{bmatrix}$$

$$\mathbf{A}_1(3) = \begin{bmatrix} 0 & 0 & 0 & 0 & 1 & 0 & 0 & 0 \\ 0 & 0 & 0 & 0 & 0 & 1 & 0 & 0 \end{bmatrix} \qquad \mathbf{B}_1(3) = \begin{bmatrix} 0 & 0 & 0 & 0 & 0 & 0 & 0 & 1 \\ 0 & 0 & 0 & 0 & 0 & 0 & -1 & 0 \end{bmatrix}$$

$$\mathbf{A}_1(4) = \begin{bmatrix} 0 & 0 & 0 & 0 & 0 & 0 & 1 & 0 \\ 0 & 0 & 0 & 0 & 0 & 0 & 0 & 1 \end{bmatrix} \qquad \mathbf{B}_1(4) = \begin{bmatrix} 0 & 0 & 0 & 0 & 0 & -1 & 0 & 0 \\ 0 & 0 & 0 & 0 & 1 & 0 & 0 & 0 \end{bmatrix}$$

$$\mathbf{A}_2(3) = \begin{bmatrix} 1 & 0 & 0 & 0 & 0 & 0 & 0 & 0 \\ 0 & 1 & 0 & 0 & 0 & 0 & 0 & 0 \end{bmatrix} \qquad \mathbf{B}_2(3) = \begin{bmatrix} 0 & 0 & 0 & 1 & 0 & 0 & 0 & 0 \\ 0 & 0 & -1 & 0 & 0 & 0 & 0 & 0 \end{bmatrix}$$

$$\mathbf{A}_2(4) = \begin{bmatrix} 0 & 0 & 1 & 0 & 0 & 0 & 0 & 0 \\ 0 & 0 & 0 & 1 & 0 & 0 & 0 & 0 \end{bmatrix} \qquad \mathbf{B}_2(4) = \begin{bmatrix} 0 & -1 & 0 & 0 & 0 & 0 & 0 & 0 \\ 1 & 0 & 0 & 0 & 0 & 0 & 0 & 0 \end{bmatrix}$$

$$\mathbf{A}_2(5) = \begin{bmatrix} 0 & 0 & 0 & 0 & 1 & 0 & 0 & 0 \\ 0 & 0 & 0 & 0 & 0 & 1 & 0 & 0 \end{bmatrix} \qquad \mathbf{B}_2(5) = \begin{bmatrix} 0 & 0 & 0 & 0 & 0 & 0 & 0 & 1 \\ 0 & 0 & 0 & 0 & 0 & 0 & -1 & 0 \end{bmatrix}$$

$$\mathbf{A}_2(6) = \begin{bmatrix} 0 & 0 & 0 & 0 & 0 & 0 & 1 & 0 \\ 0 & 0 & 0 & 0 & 0 & 0 & 0 & 1 \end{bmatrix} \qquad \mathbf{B}_2(6) = \begin{bmatrix} 0 & 0 & 0 & 0 & 0 & -1 & 0 & 0 \\ 0 & 0 & 0 & 0 & 1 & 0 & 0 & 0 \end{bmatrix}$$

$$\mathbf{A}_1(5) = \mathbf{A}_1(6) = \mathbf{A}_2(1) = \mathbf{A}_2(2) = \mathbf{B}_1(5) = \mathbf{B}_1(6) = \mathbf{B}_2(1) = \mathbf{B}_2(2) = \mathbf{0}$$

With these mapping matrices, the detailed code structure with channel coefficients can

be denoted as

$$\mathcal{X}(\mathbf{F}_i, \mathbf{x}) = \begin{bmatrix} f_{1,1}x_1 + f_{1,2}^* x_2^* & f_{1,2}x_1 - f_{1,1}^* x_2^* & & \\ -f_{1,2}^* x_1^* + f_{1,1}x_2 & f_{1,1}^* x_1^* + f_{1,2}x_2 & & \\ f_{1,1}x_3 + f_{1,2}^* x_4^* & f_{1,2}x_3 - f_{1,1}^* x_4^* & f_{2,1}x_1 + f_{2,2}^* x_2^* & f_{2,2}x_1 - f_{2,1}^* x_2^* \\ -f_{1,2}^* x_3^* + f_{1,1}x_4 & f_{1,1}^* x_3^* + f_{1,2}x_4 & -f_{2,2}^* x_1^* + f_{2,1}x_2 & f_{2,1}^* x_1^* + f_{2,2}x_2 \\ & & f_{2,1}x_3 + f_{2,2}^* x_4^* & f_{2,2}x_3 - f_{2,1}^* x_4^* \\ & & -f_{2,2}^* x_3^* + f_{2,1}x_4 & f_{2,1}^* x_3^* + f_{2,2}x_4 \end{bmatrix} \tag{4.10}$$

4.3 Diveristy Analysis with Linear Receivers

In order to analyze the diversity of the code structure proposed in the previous section, we rewrite the linear matrix equation (4.6). By substituting the block Toeplitz structure proposed in the previous section into the channel model (4.6), we can extract the transmitted symbols out and represent the pure channel matrix into a block toeplitz matrix

$$\mathbf{y}' = \boldsymbol{\mathcal{H}}\mathbf{x}' + \boldsymbol{\xi} \tag{4.11}$$

where $\mathbf{y}' = [\ y_1 \quad y_2^* \quad \cdots \quad y_{L-1} \quad y_L^*\ ]^T$, $\mathbf{x}' = [\ x_1 \quad x_2^* \quad \cdots \quad x_{K-1} \quad x_K^*\ ]^T$. During the rewriting process, we take the conjugate for the even numbered symbols, resulting in a new received vector $\mathbf{y}'$ rather than the original vector $\mathbf{y}$. The equivalent channel matrix $\boldsymbol{\mathcal{H}}$ is also a block Toeplitz matrix whose blocks are the product of two Alamouti codes:

$$\boldsymbol{\mathcal{H}} = \begin{bmatrix} \boldsymbol{\mathcal{G}}_1\boldsymbol{\mathcal{F}}_1 & & & & \\ \boldsymbol{\mathcal{G}}_2\boldsymbol{\mathcal{F}}_2 & \boldsymbol{\mathcal{G}}_1\boldsymbol{\mathcal{F}}_1 & & & \\ \boldsymbol{\mathcal{G}}_3\boldsymbol{\mathcal{F}}_3 & \boldsymbol{\mathcal{G}}_2\boldsymbol{\mathcal{F}}_2 & \ddots & & \\ \vdots & \vdots & \ddots & \ddots & \\ \boldsymbol{\mathcal{G}}_N\boldsymbol{\mathcal{F}}_N & \boldsymbol{\mathcal{G}}_{N-1}\boldsymbol{\mathcal{F}}_{N-1} & \dots & \boldsymbol{\mathcal{G}}_2\boldsymbol{\mathcal{F}}_2 & \boldsymbol{\mathcal{G}}_1\boldsymbol{\mathcal{F}}_1 \\ & \boldsymbol{\mathcal{G}}_N\boldsymbol{\mathcal{F}}_N & \dots & \boldsymbol{\mathcal{G}}_3\boldsymbol{\mathcal{F}}_3 & \boldsymbol{\mathcal{G}}_2\boldsymbol{\mathcal{F}}_2 \\ & & \ddots & \vdots & \vdots \\ & & & \boldsymbol{\mathcal{G}}_N\boldsymbol{\mathcal{F}}_N & \boldsymbol{\mathcal{G}}_{N-1}\boldsymbol{\mathcal{F}}_{N-1} \\ & & & & \boldsymbol{\mathcal{G}}_N\boldsymbol{\mathcal{F}}_N \end{bmatrix} \in \mathbb{C}^{(K+2N-2)\times 2N} \quad (4.12)$$

The 2×2 block in $\boldsymbol{\mathcal{H}}$ is the product of two Alamouti code, whose elements are the channel coefficients of the two transmission phases, respectively, i.e.

$$\boldsymbol{\mathcal{G}}_j = \begin{bmatrix} g_{j1} & -g_{j2} \\ g_{j2}^* & g_{j1}^* \end{bmatrix} \quad \text{and} \quad \boldsymbol{\mathcal{F}}_j = \begin{bmatrix} f_{j1} & f_{j2}^* \\ -f_{j2} & f_{j1}^* \end{bmatrix} \quad (4.13)$$

Lemma 1. *The matrix $\boldsymbol{\mathcal{H}}$ has full column rank, if at least one of the N product channel is nonzero, i.e. $\sum_{i=1}^{N} \|\mathbf{g}_i\|^2\|\mathbf{f}_i\|^2 \neq 0$.*

Proof. The equivalent channel matrix $\boldsymbol{\mathcal{H}}$ is a block Toeplitz matrix, whose blocks are the product of two Alamouti codes.

$$\boldsymbol{\mathcal{G}}_j\boldsymbol{\mathcal{F}}_j = \begin{bmatrix} g_{j1} & -g_{j2} \\ g_{j2}^* & g_{j1}^* \end{bmatrix} \begin{bmatrix} f_{j1} & f_{j2}^* \\ -f_{j2} & f_{j1}^* \end{bmatrix} \quad (4.14)$$

The product of Alamouti code is full rank if $\|\mathbf{g}_j\|^2\|\mathbf{f}_j\|^2 \neq 0$.

$$\begin{aligned}
&\boldsymbol{\mathcal{F}}_j^H \boldsymbol{\mathcal{G}}_j^H \boldsymbol{\mathcal{G}}_j \boldsymbol{\mathcal{F}}_j = \boldsymbol{\mathcal{G}}_j \boldsymbol{\mathcal{F}}_j \boldsymbol{\mathcal{F}}_j^H \boldsymbol{\mathcal{G}}_j^H \\
&= \begin{bmatrix} f_{j1}^* & -f_{j2}^* \\ f_{j2} & f_{j1} \end{bmatrix} \begin{bmatrix} g_{j1}^* & g_{j2} \\ -g_{j2}^* & g_{j1} \end{bmatrix} \begin{bmatrix} g_{j1} & -g_{j2} \\ g_{j2}^* & g_{j1}^* \end{bmatrix} \begin{bmatrix} f_{j1} & f_{j2}^* \\ -f_{j2} & f_{j1}^* \end{bmatrix} \\
&= \|\mathbf{g}_j\|^2 \|\mathbf{f}_j\|^2 \mathbf{I}_2
\end{aligned} \tag{4.15}$$

The proof process is very straightforward. Let's check the upper square matrix first, which is a lower triangular matrix whose diagonal values are $\boldsymbol{\mathcal{G}}_1\boldsymbol{\mathcal{F}}_1$. If $\boldsymbol{\mathcal{G}}_1\boldsymbol{\mathcal{F}}_1$ is nonzero, it's sufficient that the lower triangular matrix is full rank, so is the equivalent matrix $\boldsymbol{\mathcal{H}}$. If $\boldsymbol{\mathcal{G}}_1\boldsymbol{\mathcal{F}}_1 = 0$, we can repetitively check the $\boldsymbol{\mathcal{G}}_2\boldsymbol{\mathcal{F}}_2$, $\boldsymbol{\mathcal{G}}_3\boldsymbol{\mathcal{F}}_3$ and the square matrix beginning from an even numbered row, which is also a lower triangular matrix whose diagonal blocks are $\boldsymbol{\mathcal{G}}_i\boldsymbol{\mathcal{F}}_i$. If $\boldsymbol{\mathcal{G}}_i\boldsymbol{\mathcal{F}}_i \neq 0$, the lower triangular matrix is full rank.

Since we have the prerequisite that $\sum_{i=1}^{N} \|\mathbf{g}_i\|^2 \|\mathbf{f}_i\|^2 \neq 0$, at least one block $\boldsymbol{\mathcal{G}}_i\boldsymbol{\mathcal{F}}_i$ is nonzero. Therefore, when we analyzing in this procedure, at least one lower triangular matrix specified in the previous paragraph is full rank, so is the equivalent matrix $\boldsymbol{\mathcal{H}}$.

□

Lemma 2. *The determinant of $\boldsymbol{\mathcal{H}}^H\boldsymbol{\mathcal{H}}$ has the following lower and upper bound.*

$$C_{\min} \left\{ \sum_{j=1}^{N} \|\mathbf{g}_j\|^2 \|\mathbf{f}_j\|^2 \right\}^N \leq \det\left(\boldsymbol{\mathcal{H}}^H\boldsymbol{\mathcal{H}}\right) \leq C_{\max} \left\{ \sum_{j=1}^{N} \|\mathbf{g}_j\|^2 \|\mathbf{f}_j\|^2 \right\}^N, \tag{4.16}$$

where $C_{\min}$ and $C_{\max}$ are nonzero constants independent of the channel coefficients.

Proof. In order to analyze the columns of $\boldsymbol{\mathcal{H}}$, we first analyze the 2-norm of each column. Each pair of columns has all of the blocks of $\boldsymbol{\mathcal{F}}_i^H \boldsymbol{\mathcal{G}}_i^H$, where i is from 1 to N.

The 2-norm of each column is the same as that of $\begin{bmatrix} \boldsymbol{\mathcal{F}}_1^T\boldsymbol{\mathcal{G}}_1^T & \boldsymbol{\mathcal{F}}_2^T\boldsymbol{\mathcal{G}}_2^T & \cdots & \boldsymbol{\mathcal{F}}_N^T\boldsymbol{\mathcal{G}}_N^T \end{bmatrix}^T$.

$$\begin{bmatrix} \boldsymbol{\mathcal{F}}_1^H\boldsymbol{\mathcal{G}}_1^H & \boldsymbol{\mathcal{F}}_2^H\boldsymbol{\mathcal{G}}_2^H & \cdots & \boldsymbol{\mathcal{F}}_N^H\boldsymbol{\mathcal{G}}_N^H \end{bmatrix} \begin{bmatrix} \boldsymbol{\mathcal{G}}_1\boldsymbol{\mathcal{F}}_1 \\ \boldsymbol{\mathcal{G}}_2\boldsymbol{\mathcal{F}}_2 \\ \vdots \\ \boldsymbol{\mathcal{G}}_N\boldsymbol{\mathcal{F}}_N \end{bmatrix} = \sum_{i=1}^{N} \|\mathbf{g}_j\|^2\|\mathbf{f}_j\|^2\mathbf{I}_2 \tag{4.17}$$

Therefore, each column of $\boldsymbol{\mathcal{H}}$ has the same 2-norm of $\sqrt{\sum_{i=1}^{N} \|\mathbf{g}_j\|^2\|\mathbf{f}_j\|^2}$. If extracting the 2-norm from each column, we will arrive at a matrix whose columns all have unit 2-norm, denoted as $\bar{\boldsymbol{\mathcal{H}}}$.

$$\boldsymbol{\mathcal{H}} = \sqrt{\sum_{i=1}^{N} \|\mathbf{g}_j\|^2\|\mathbf{f}_j\|^2} \cdot \bar{\boldsymbol{\mathcal{H}}} \tag{4.18}$$

The determinant can be represented with the unit-column-norm matrix $\bar{\boldsymbol{\mathcal{H}}}$.

$$\det\left(\boldsymbol{\mathcal{H}}^H\boldsymbol{\mathcal{H}}\right) = \left\{\sum_{i=1}^{N} \|\mathbf{g}_j\|^2\|\mathbf{f}_j\|^2\right\}^N \det\left(\bar{\boldsymbol{\mathcal{H}}}^H\bar{\boldsymbol{\mathcal{H}}}\right) \tag{4.19}$$

Since each column of $\bar{\boldsymbol{\mathcal{H}}}$ has the same norm, the determinant of positive semidefinite (PSD) matrix $\bar{\boldsymbol{\mathcal{H}}}^H\bar{\boldsymbol{\mathcal{H}}}$ is continuous in a closed bounded feasible set $\{\bar{\boldsymbol{\mathcal{H}}} : \|\bar{\boldsymbol{\mathcal{H}}}^{(j)}\| = 1\}$, where $\bar{\boldsymbol{\mathcal{H}}}^{(j)}$ is the jth column of $\bar{\boldsymbol{\mathcal{H}}}$. $\bar{\boldsymbol{\mathcal{H}}}$ is also full rank from Lemma 1. The determinant can be bounded by two nonzero constants $C_{\min}$ and $C_{\max}$, i.e. $C_{\min} \leq \det\left(\bar{\boldsymbol{\mathcal{H}}}^H\bar{\boldsymbol{\mathcal{H}}}\right) \leq C_{\max}$. Therefore, the determinant of $\boldsymbol{\mathcal{H}}^H\boldsymbol{\mathcal{H}}$ is also bounded by the

polynomials below.

$$C_{\min}\left\{\sum_{j=1}^{N}\|\mathbf{g}_j\|^2\|\mathbf{f}_j\|^2\right\}^N \leq \det\left(\boldsymbol{\mathcal{H}}^H\boldsymbol{\mathcal{H}}\right) \leq C_{\max}\left\{\sum_{j=1}^{N}\|\mathbf{g}_j\|^2\|\mathbf{f}_j\|^2\right\}^N \tag{4.20}$$

□

With the two intermediate lemmas above, we arrive at the following lemma.

Lemma 3. *For the block Toeplitz structure proposed, the diagonal elements of* $[\boldsymbol{\mathcal{H}}^H\boldsymbol{\mathcal{H}}]^{-1}$ *satisfie the following inequality:*

$$\left[(\boldsymbol{\mathcal{H}}^H\boldsymbol{\mathcal{H}})^{-1}\right]_{k,k}^{-1} \geq C_0\left\{\sum_{j=1}^{N}\|\mathbf{g}_j\|^2\|\mathbf{f}_j\|^2\right\}, \tag{4.21}$$

where C_0 *is a constant independent of the channel coefficients.*

Proof. From the matrix inversion properties [39], we have

$$\left[(\boldsymbol{\mathcal{H}}^H\boldsymbol{\mathcal{H}})^{-1}\right]_{k,k}^{-1} = \frac{\det\left(\boldsymbol{\mathcal{H}}^H\boldsymbol{\mathcal{H}}\right)}{\det\left(\boldsymbol{\mathcal{H}}_k^H\boldsymbol{\mathcal{H}}_k\right)}, \tag{4.22}$$

where $\boldsymbol{\mathcal{H}}_k$ is a matrix obtained by removing the kth column of $\boldsymbol{\mathcal{H}}$. We can see that $\boldsymbol{\mathcal{H}}_k^H\boldsymbol{\mathcal{H}}_k$ is still nonsingular and PSD, thus satisfying the Lemma 2. $\det\left(\boldsymbol{\mathcal{H}}_k^H\boldsymbol{\mathcal{H}}_k\right)$ has a upper bound denoted by $C_{k\max}\left\{\sum_{j=1}^{N}\|\mathbf{g}_j\|^2\|\mathbf{f}_j\|^2\right\}^{N-1}$. Therefore, the theorem can be proved.

$$\left[(\boldsymbol{\mathcal{H}}^H\boldsymbol{\mathcal{H}})^{-1}\right]_{k,k}^{-1} \geq \frac{C_{\min}\left\{\sum_{j=1}^{N}\|\mathbf{g}_j\|^2\|\mathbf{f}_j\|^2\right\}^N}{C_{k\max}\left\{\sum_{j=1}^{N}\|\mathbf{g}_j\|^2\|\mathbf{f}_j\|^2\right\}^{N-1}} = C_0\left\{\sum_{j=1}^{N}\|\mathbf{g}_j\|^2\|\mathbf{f}_j\|^2\right\}, \tag{4.23}$$

where $C_0 = C_{\min}/C_{k\max}$. □

The noise received at the destination node is the addition of two parts: one part from the relay nodes multiplied by the channel coefficients, and the other parts from the destination node when receiving. Due to the mapping matrices at the relay nodes, the noise expression also has the same block Toeplitz structure as (4.7), represented in the following expression.

$$\boldsymbol{\xi} = \begin{bmatrix} \boldsymbol{\mathcal{N}}_1(1,2) & & & & & \\ \boldsymbol{\mathcal{N}}_1(3,4) & \boldsymbol{\mathcal{N}}_2(1,2) & & & & \\ \boldsymbol{\mathcal{N}}_1(5,6) & \boldsymbol{\mathcal{N}}_2(3,4) & \ddots & & & \\ \vdots & \vdots & \ddots & \ddots & & \\ \boldsymbol{\mathcal{N}}_1(K-1,K) & \boldsymbol{\mathcal{N}}_2(K-3,K-2) & \dots & \boldsymbol{\mathcal{N}}_{N-1}(3,4) & \boldsymbol{\mathcal{N}}_N(1,2) & \\ & \boldsymbol{\mathcal{N}}_2(K-1,K) & \dots & \boldsymbol{\mathcal{N}}_{N-1}(5,6) & \boldsymbol{\mathcal{N}}_N(3,4) & \\ & & \ddots & \vdots & \vdots & \\ & & & \boldsymbol{\mathcal{N}}_{N-1}(K-1,K) & \boldsymbol{\mathcal{N}}_N(K-3,K-2) & \\ & & & & \boldsymbol{\mathcal{N}}_N(K-1,K) & \end{bmatrix} \begin{bmatrix} \mathbf{g}_1 \\ \mathbf{g}_2 \\ \vdots \\ \mathbf{g}_N \end{bmatrix} + \boldsymbol{\eta} \tag{4.24}$$

and

$$\boldsymbol{\mathcal{N}}_i(k,l) = \begin{bmatrix} n_{i1}(k) + n_{i2}^*(l) & n_{i2}(k) - n_{i1}^*(l) \\ -n_{i2}^*(k) + n_{i1}(l) & n_{i1}^*(k) + n_{i2}(l) \end{bmatrix} \tag{4.25}$$

As is shown in the equation above, the block Toeplitz matrix is not filled with the blocks $\boldsymbol{\mathcal{N}}_i(k,l)$, meaning that the overall noise is not white in this model. In order to analyze the SEP, we use the upper bound of the noise covariance matrix for calculation, i.e. $\mathbf{R} \leq \mathbb{E}[\boldsymbol{\xi}\boldsymbol{\xi}^H] \preceq \sigma^2(1 + 2\sum_{i=1}^{N} \|\mathbf{g}_i\|^2)\mathbf{I}$.

The suboptimal linear SBSD is also employed in order to maintain a lower detection complexity. When we multiply (4.11) by the pseudo inverse of $\boldsymbol{\mathcal{H}}$, we can have the following linear receiver.

$$\tilde{\mathbf{y}} = \mathbf{x}' + (\boldsymbol{\mathcal{H}}^H\boldsymbol{\mathcal{H}})^{-1}\boldsymbol{\mathcal{H}}^H\boldsymbol{\xi} \tag{4.26}$$

Please note that since the overall noise is not white, then detection performance of multiplying the pseudo inverse of the channel matrix is actually worse than that of ZF receiver. After multiplying the pseudo inverse of the channel matrix, the overall noise in the expression above is still not white. The covariance matrix can be upper bounded by

$$\tilde{\mathbf{R}} = (\boldsymbol{\mathcal{H}}^H\boldsymbol{\mathcal{H}})^{-1}\boldsymbol{\mathcal{H}}^H\mathbb{E}[\boldsymbol{\xi}\boldsymbol{\xi}^H]\boldsymbol{\mathcal{H}}(\boldsymbol{\mathcal{H}}^H\boldsymbol{\mathcal{H}})^{-1} \preceq \sigma^2(1+2\sum_{i=1}^{N}\|\mathbf{g}_i\|^2)(\boldsymbol{\mathcal{H}}^H\boldsymbol{\mathcal{H}})^{-1}. \quad (4.27)$$

Theorem 3. *The Alamouti Based Toeplitz Space-Time Block Code structure proposed can achieve the optimal diversity function $\frac{\ln^N\rho}{\rho^{2N}}$, when square QAM constellation and linear symbol-by-symbol receiver are employed.*

Proof. See appendix A. □

With the code structure we proposed, the linear SBSD could achieve both the optimal diversity function and lower detection computational complexity.

Chapter 5

Numerical Results

In this chapter, the theorems and principles proposed in the previous two chapters are verified through Monte Carlo simulation method. In the simulation process, the channel coefficients are all assumed to be *i.i.d.* zero-mean circular symmetric complex Gaussian variables with unit variance and the noise variables are also *i.i.d.* zero-mean circular symmetric complex Gaussian variables. The transmitted symbols are randomly chosen from a quantized square 16-QAM constellation and different symbols are chosen independently. The symbol rate is defined as the number of symbols transmitted per time slot used in the second phase. For example, Rate-2/4 means two symbols are transmitted in the two-phase transmission process and four time slots are utilized in the second phase. The performance evaluation is based on both BER and SEP.

5.1 Simulation Results of ODSTBC

For this code structure, several scenarios are verified:

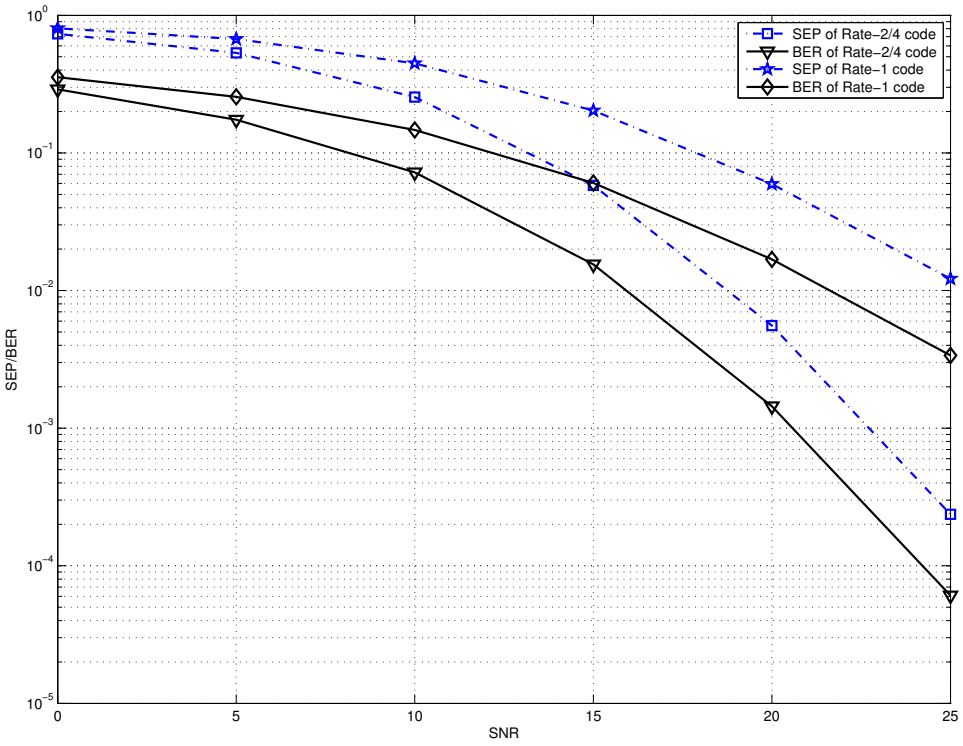

Figure 5.1: SEP/BER performance of Rate-1 code and Rate-2/4 code

1. Two distributed single antenna relays

2. Four distributed single antenna relays

3. The comparison of theoretical results from Theorem 2 with numerical results

4. The comparison of performance of the code structure proposed in this thesis with that of the code structure $\mathcal{X}(4,4)$ proposed in [18]

Figure 5.1 is the error performance, in terms of BER and SEP, of Rate-1 code and Rate-2/4 code with 2 distributed relay stations and 4 relay stations, respectively.

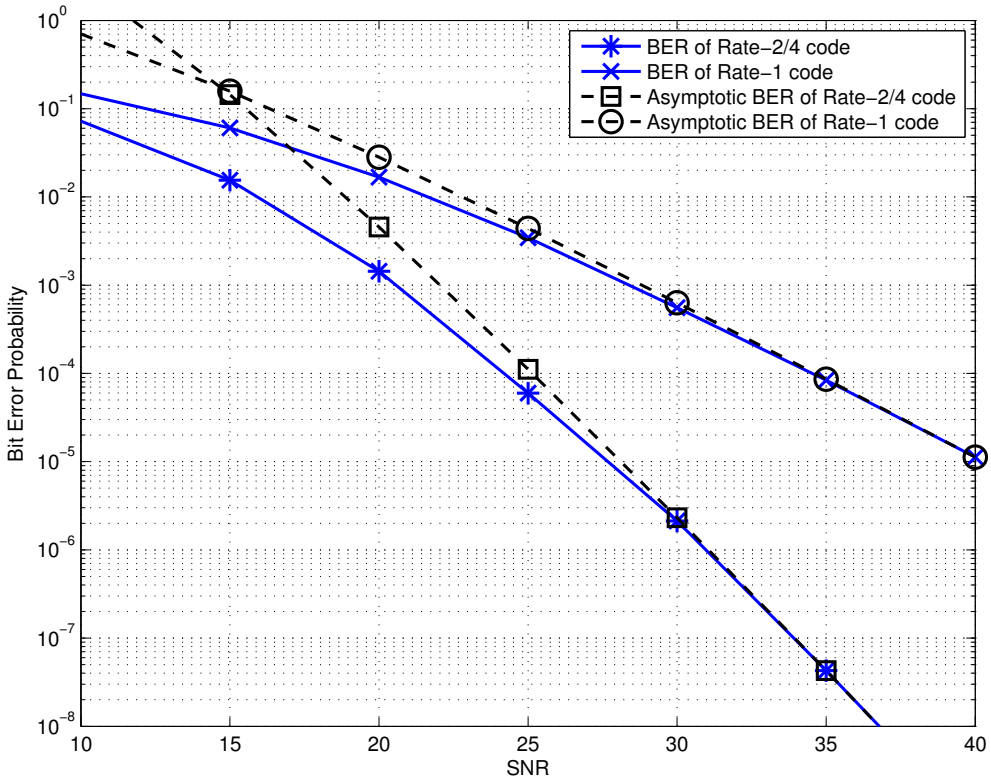

Figure 5.2: BER performance comparison of Rate-1 and Rate-2/4 orthogonal design

Both SEP and BER of the two channel models are simulated. As is illustrated in the figure, we could see that both of the curves achieve their optimal diversity function of $\left(\frac{\ln \rho}{\rho}\right)^2$ and $\left(\frac{\ln \rho}{\rho}\right)^4$, respectively. As SNR increases, Rate-2/4 code performs much better than Rate-1 code, as is expected with the higher asymptotical diversity order.

The comparison of theoretical result in Theorem 2 with the numerical results is shown in Figure 5.2. Since the error formula in Theorem 2 only keeps the dominant term of the optimal diversity function, the theoretical SEP is not accurate when SNR is relatively low. But when SNR is sufficiently large, the theoretical SEP curves converge to the numerical results, which verified the correctness of the result. The

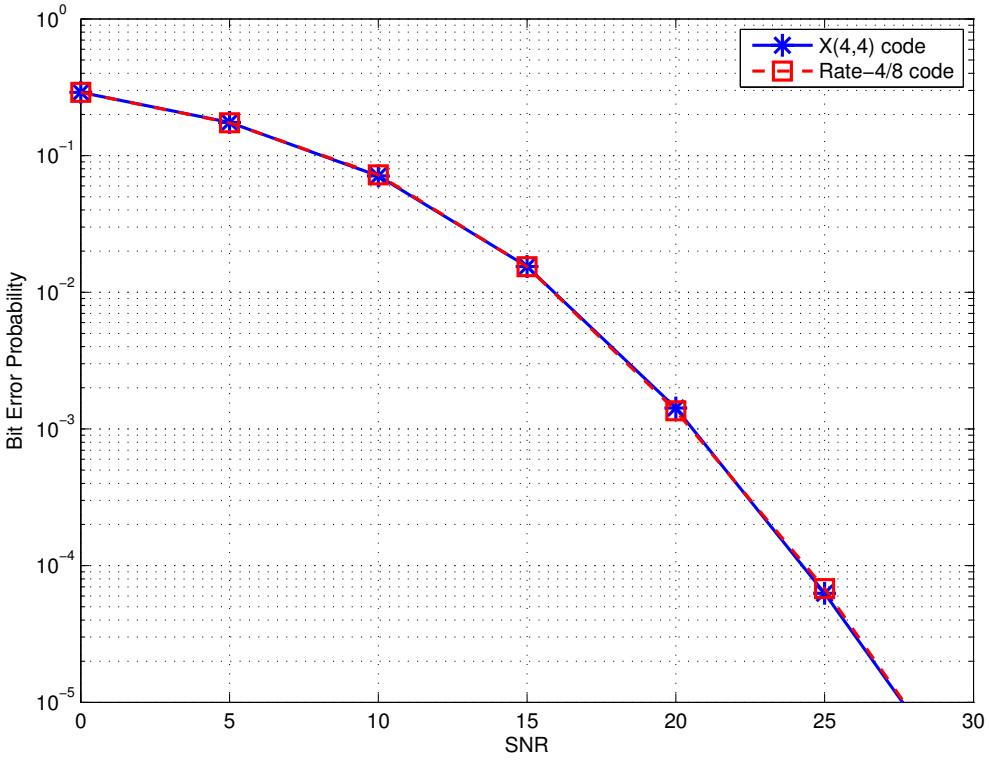

Figure 5.3: BER performance comparison of Rate-2/4 orthogonal design and X(4,4) code in [18]

code structure proposed in this paper is also compared to that in [18], which proposed a similar code structure from a different perspective. Both of these two code structures could achieve the same diversity function of $\frac{\ln^N \rho}{\rho^N}$. Therefore, the SEP performance of Rate-2/4 code and the $\mathcal{X}(4,4)$ proposed in [18] are really similar, shown in Figure 5.3. But the code structure proposed here enjoys much lower computation complexity with the symbol-by-symbol detection.

5.2 Simulation Results of ABTSTBC

The numerical performance of ABTSTBC is verified in this section. The number of symbols transmitted in one two-phase transmission process is chosen as K. The number of time slots used in the first and second phase are K and L, respectively. Due to the structure of the block Toeplitz code, $L = K + 2N - 2$. Therefore, the (relative) symbol rate is $\frac{K}{K+2N-2}$. As K increases, the symbol rate approaches to 1, which is the upper bound of the maximum symbol rate. This is also one of the advantages of the code structure. The data rate will not decrease dramatically when the number of antennas increases, which is desirable in systems with large number of relays and antennas. The SEP and BER performance of the code when two two-antenna relays are deployed is presented in Figure 5.4, while Figure 5.5 is the SEP and BER performance when three two-antenna relays are deployed. The performance comparison of these two structure is provided in Figure 5.6. When the SNR is relatively low, there is no big difference between the performance of the two code structures. However, as SNR increases, the BER performance of three relays is better due to the diversity function of $\frac{\ln^3 \rho}{\rho^6}$ compared to the diversity of $\frac{\ln^2 \rho}{\rho^4}$ with two relays. Therefore, when more number of relays are delayed, the system could achieve higher asymptotic

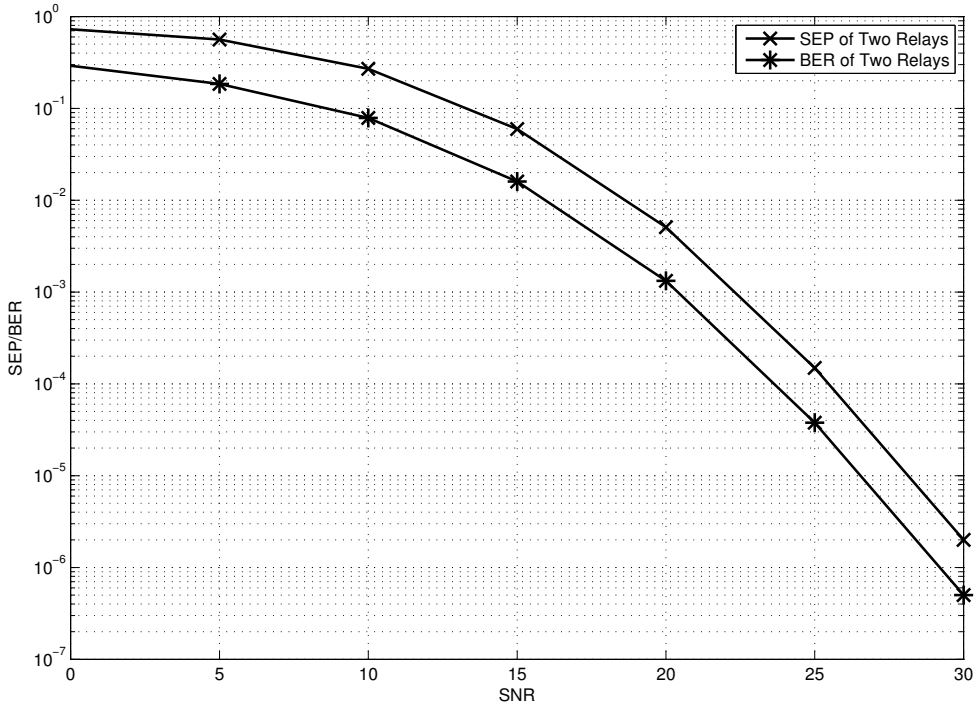

Figure 5.4: SEP/BER performance of two two-antenna relays

diversity order without sacrificing the overall symbol rate.

Figure 5.7 is the comparison of ABTSTBC with ODSTBC. The systems for the two code structures are equipped with two two-antenna relays and four single antenna relays, respectively. As is shown in Theorem 2 and Theorem 3, the ABTSTBC has a optimal diversity of $\frac{\ln^2 \rho}{\rho^4}$ while ODSTBC has the diversity function of $\frac{\ln^4 \rho}{\rho^4}$. The performance reflects the difference. The ABTSTBC has a better performance compared with ODSTBC due to lower order of the factor $\ln \rho$. When the SNR is relatively high, the two curves tend to be parallel with each other, which achieves the same asymptotic full diversity order of 4. However, the ABTSTBC still enjoys better BER performance due to lower order of the factor $\ln \rho$.

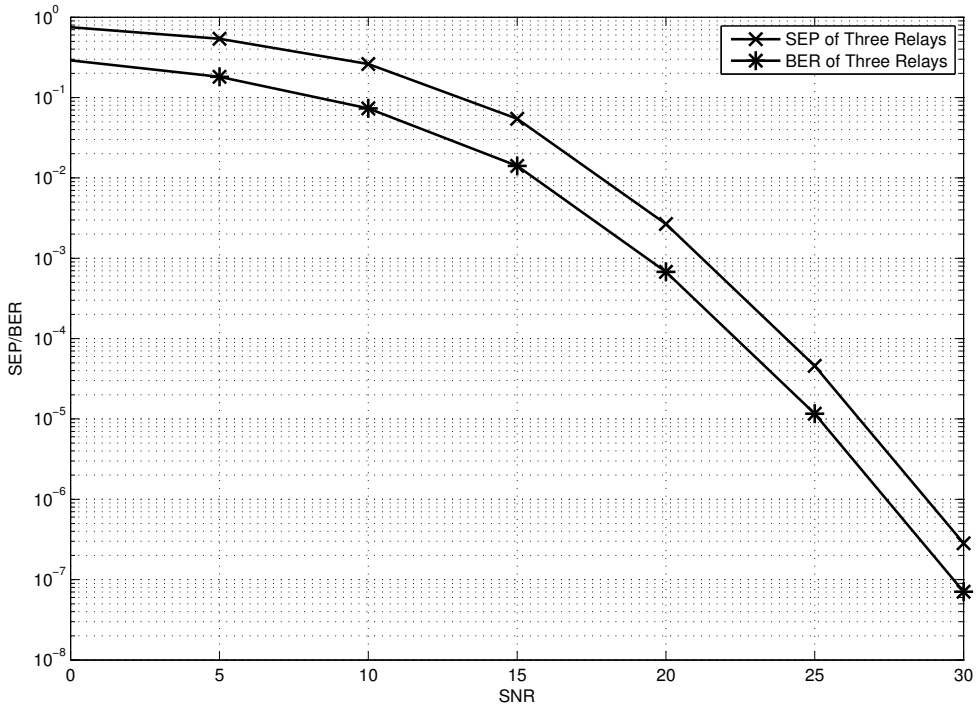

Figure 5.5: SEP/BER performance of three two-antenna relays

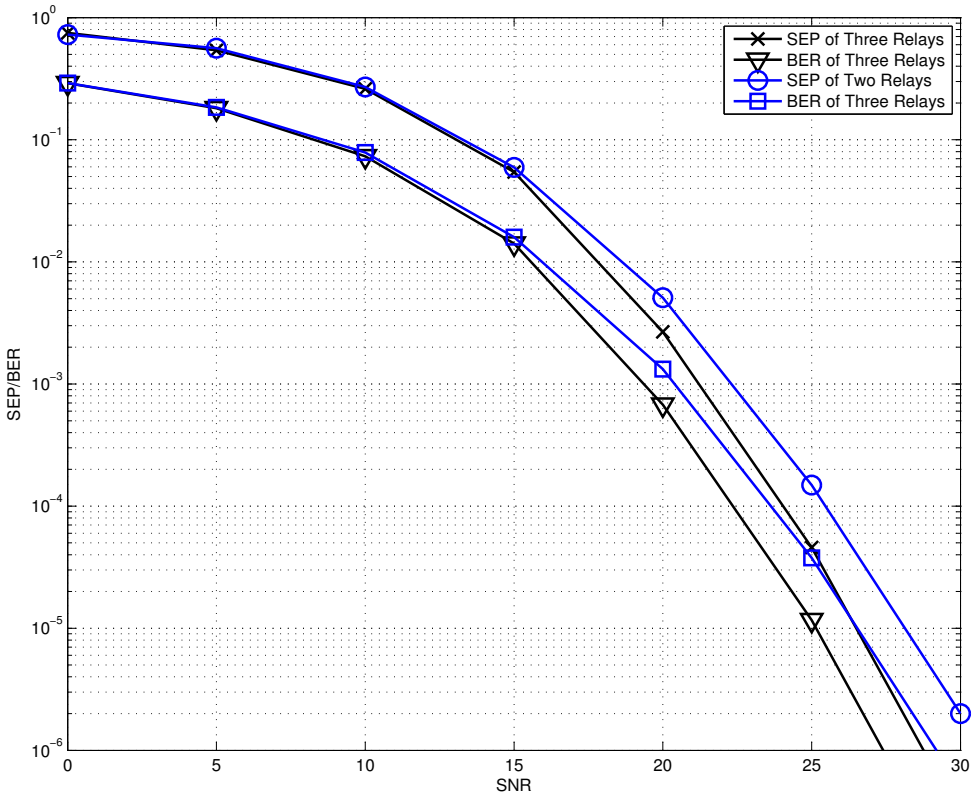

Figure 5.6: SEP/BER performance comparison of two and three two-antenna relays

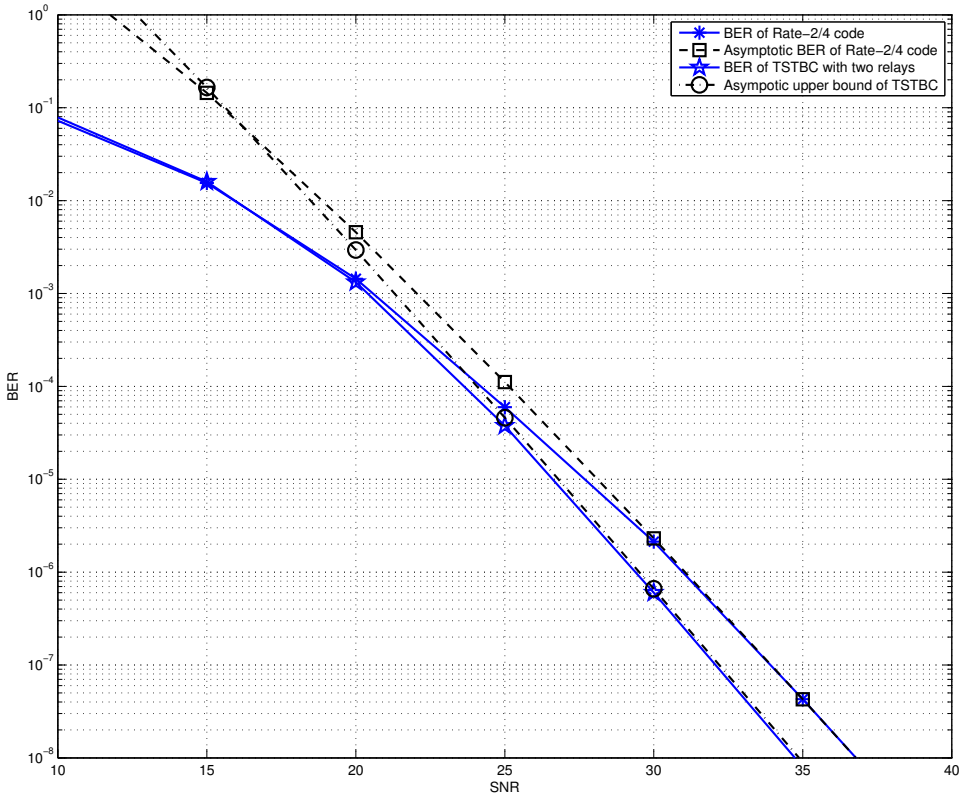

Figure 5.7: BER performance comparison of ODSTBC (four single antenna relays) with ABTSTBC (two two-antenna relays)

Chapter 6

Conlusions and Future Work

6.1 Conlusions

In this thesis, two Space-Time Block Code structures are proposed: Orthogonally-Distributed Space-Time Codes (ODSTBC) for single antenna distributed relay channels and Alamouti Based Toeplitz Space-Time Block Codes (ABTSTBC) for two-antenna distributed relay channels.

The first orthogonal STBC maintains the orthogonality in single antenna distributed relay channels as OSTBC does in MIMO channels. The orthogonality of ODSTBC guarantees the optimal diversity function $\frac{\ln^N \rho}{\rho^N}$, optimal coding gain and works well when the number of relays is the power of 2. Two design code schemes are provided, which maintain the orthogonal conditions and achieves equivalent optimal ML detection performance. However, due to the strict orthogonal conditions of the codes, the (relative) symbol rate is relative low, i.e. 2^{1-n}, where 2^n is the number of relays. When the number of relays increases, the symbol rate will decrease dramatically, which is undesirable in practical systems.

In order to relieve the low symbol rate dilemma, we deploy more antennas and eliminate the orthogonal conditions, thus resulting in the Alamouti Based Toeplitz STBC. The ABTSTBC employs a block Toeplitz structure both in the code structure and in the equivalent channel matrix. The code structure consists of blocks which are the addition of two Alamouti code, while the equivalent channel matrix consists of blocks which are the product of two Alamouti channel coefficients. The Toeplitz structure guarantees the full rank and thus the optimal diversity function $\frac{\ln^N \rho}{\rho^{2N}}$ is achieved. Due to the cooperations between each antenna pair of each relay, the performance of this algorithm is better than that of the single antenna relays, whose diversity function is $\frac{\ln^N \rho}{\rho^N}$, in terms of both SEP and BER. The ABTSTBC also utilizes a linear symbol-by-symbol receiver to maintain a lower computational complexity.

6.2 Future Work

With the current results of the thesis, some advantageous code structures have been achieved. However, there is still room to improve the current results. Some possible aspects to work on are listed in the following.

- For the ODSTBC, two design patterns are provided, whose performance is equivalent to the ML detection in the current channel setup. Some more designs need to be verified to see whether these two structures accidentally achieve the ML performance or any design fulfilling the orthogonal conditions are equivalent to the ML detection performance.

- The current symbol rate of ODSTBC for single antenna relay channels is relative low. Some future work should cover the orthogonal design of multiple

antenna relay channels. If there are orthogonal designs for multiple antenna relay channels, the optimal coding gain, diversity function and low computation complexity might be achieve simultaneously.

- The current design of ABTSTBC achieves the optimal diversity function and low complexity with linear symbol-by-symbol detection. However, in the Toeplitz matrix, some entries remain zero, which means that the space and time are not fully utilized. Future work may address in designing some block circular matrices, making the most of the space and time freedom.

- The noise for the ABTSTBC structure is not white. Therefore, the symbol-by-symbol linear detection method is not optimal as ML detection in this model. Some work needs to address the noise properties, designing code structures which fully utilize the space and time freedom and make the overall noise white. With white noise, the symbol-by-symbol detection would be equivalent to the optimal ML detection.

Appendix A

A.1 Proof of Theorem 2

Proof. Note that since $\mathbf{A}_n^H\mathbf{A}_n+\mathbf{B}_n^T\mathbf{B}_n^* = \mathbf{I}$, and $L \geq K$, we have $\mathbf{0} \preceq \mathbf{A}_n\mathbf{A}_n^H+\mathbf{B}_n\mathbf{B}_n^H \preceq \mathbf{I}$ and thus, $\sigma^2\|\mathbf{h}\|^2\mathbf{I} \preceq \tilde{\mathbf{R}} \preceq \sigma^2(1+\|\mathbf{g}\|^2)\|\mathbf{h}\|^2\mathbf{I}$. The SEP of SBSD for the square M-ary QAM constellation is upper and lower bounded by

$$\mathrm{P}_{\mathrm{SEP}} \leq \mathrm{P}_1 = 4\left(1-\frac{1}{\sqrt{M}}\right)\mathcal{Q}_1 - 4\left(1-\frac{1}{\sqrt{M}}\right)^2\mathcal{Q}_1^2, \tag{A.1a}$$

$$\mathrm{P}_{\mathrm{SEP}} \geq \mathrm{P}_2 = 4\left(1-\frac{1}{\sqrt{M}}\right)\mathcal{Q}_2 - 4\left(1-\frac{1}{\sqrt{M}}\right)^2\mathcal{Q}_2^2, \tag{A.1b}$$

where $\mathcal{Q}_1 = \mathrm{Q}\left(\frac{\|\mathbf{h}\|d}{\sigma\sqrt{2(1+\|\mathbf{g}\|^2)}}\right)$, $\mathcal{Q}_2 = \mathrm{Q}\left(\frac{\|\mathbf{h}\|d}{\sqrt{2}\sigma}\right)$, and $\mathrm{Q}(\cdot)$ is the *Q-function*, whose alternative expression is $\mathrm{Q}(x) = \frac{1}{\pi}\int_0^{\frac{\pi}{2}}\exp\left(-\frac{x^2}{2\sin^2\theta}\right)\mathrm{d}\theta$, where $d = \sqrt{\frac{6E_s}{M-1}}$ is the minimum distance in the square QAM constellation and E_s is the average symbol energy. The SER above will vary as the realization of f_n and g_n vary. In order to have a evaluation of the system, we need to calculate the expectation of the SER expression above with respect to all possible values of f_n and g_n, $n = 1, ..., N$. With the alternative expression of *Q-function*, i.e. $\mathrm{Q}(x) = \dfrac{1}{\pi}\displaystyle\int_0^{\frac{\pi}{2}}\exp\left(-\frac{x^2}{2\sin^2\theta}\right)\mathrm{d}\theta$, the

Q-function above can be represented as

$$\mathcal{Q}_1 = \mathrm{Q}\left(\frac{\|\mathbf{h}\|d}{\sigma\sqrt{2(1+\|\mathbf{g}\|^2)}}\right) = \frac{1}{\pi}\int_0^{\frac{\pi}{2}} \exp\left(-\frac{\|\mathbf{h}\|^2 d^2}{4\sigma^2(1+\|\mathbf{g}\|^2)\sin^2\theta}\right)\mathrm{d}\theta \tag{A.2}$$

Based on the assumption that the channel coefficients f_n and g_n are *i.i.d* circular complex Gaussian random variable with unit variance, the probability density functions of $|f_n|^2$ and $|g_n|^2$ are all $\mathrm{p}(t) = \exp(-t)$. Since the channel coefficients of two transmission phases are independent, we can take the expectation with regard to $\mathbf{f}$ and $\mathbf{g}$ in two steps, separately, i.e. $\mathbb{E}_{\mathbf{f},\mathbf{g}}[\cdot] = \mathbb{E}_{\mathbf{g}}\left\{\mathbb{E}_{\mathbf{f}}[\cdot]\right\}$.

In the first step, we calculate the expectation with regards to $\mathbf{f}$.

$$\mathbb{E}_{\mathbf{f},\mathbf{g}}\left[\mathrm{Q}\left(\frac{\|\mathbf{h}\|d}{\sigma\sqrt{2(1+\|\mathbf{g}\|^2)}}\right)\right] = \frac{1}{\pi}\int_0^{\frac{\pi}{2}} \mathbb{E}\left[\exp\left(-\frac{\|\mathbf{h}\|^2 d^2}{4\sigma^2(1+\|\mathbf{g}\|^2)\sin^2\theta}\right)\right]\mathrm{d}\theta \tag{A.3}$$

$$\begin{aligned}\mathbb{E}_{\mathbf{f}}\left[\exp\left(-\frac{\|\mathbf{h}\|^2 d^2}{4\sigma^2(1+\|\mathbf{g}\|^2)\sin^2\theta}\right)\right] &= \mathbb{E}_{\mathbf{f}}\left[\exp\left(-\frac{\sum_{n=1}^{N}|f_n|^2|g_n|^2 d^2}{4\sigma^2(1+\|\mathbf{g}\|^2)\sin^2\theta}\right)\right] \\ &= \prod_{n=1}^{N}\mathbb{E}_{f_n}\left[\exp\left(-\frac{|f_n|^2|g_n|^2 d^2}{4\sigma^2(1+\|\mathbf{g}\|^2)\sin^2\theta}\right)\right]\end{aligned} \tag{A.4}$$

As we assumed at the beginning of this article, the channel coefficients h_n and g_n are *i.i.d.* Circular Symmetric Complex Gaussian variable with unit variance. Therefore, the product in the equation above can be calculated independently.

$$\mathbb{E}_{f_n}\left[\exp\left(-\frac{|f_n|^2|g_n|^2 d^2}{4\sigma^2(1+\|\mathbf{g}\|^2)\sin^2\theta}\right)\right] = \int_0^{\infty}\exp\left(-\frac{t|g_n|^2 d^2}{4\sigma^2(1+\|\mathbf{g}\|^2)\sin^2\theta} - t\right)\mathrm{d}t = \frac{1+\|\mathbf{g}\|^2}{1+\|\mathbf{g}\|^2+\frac{|g_n|^2 d^2}{4\sigma^2\sin^2\theta}} \tag{A.5}$$

In the second step, we calculate the expectation with regards to $\mathbf{g}$. Since the residue of the expression above is rather complicated, the expectation with respect to each g_k is difficult to calculate. Therefore, we rewrite the expression and calculate

a upper bound of the SER.

$$\begin{aligned}&\mathbb{E}\left[\exp\left(-\frac{\|\mathbf{h}\|^2 d^2}{4\sigma^2(1+\|\mathbf{g}\|^2)\sin^2\theta}\right)\right] = \mathbb{E}_{\mathbf{g}}\left[\prod_{n=1}^{N}\frac{1+\|\mathbf{g}\|^2}{1+\|\mathbf{g}\|^2+\frac{|g_n|^2 d^2}{4\sigma^2\sin^2\theta}}\right]\\ \leq&\mathbb{E}_{\mathbf{g}}\left[\prod_{n=1}^{N}\frac{1+\|\mathbf{g}\|^2}{1+\frac{|g_n|^2 d^2}{4\sigma^2\sin^2\theta}}\right] = \mathbb{E}_{\mathbf{g}}\left[\frac{(1+\sum_{n=1}^{N}|g_n|^2)^N}{\prod_{n=1}^{N}\left(1+\frac{|g_n|^2 d^2}{4\sigma^2\sin^2\theta}\right)}\right]\end{aligned} \tag{A.6}$$

The expectation above is a N dimensional (N-D) integral with regards to all $|g_n|^2, n = 1, 2, ..., N$, whose pdf are all $p(t) = \exp(-t)$.

$$\mathbb{E}_{\mathbf{g}}\left[\frac{(1+\sum_{n=1}^{N}|g_n|^2)^N}{\prod_{n=1}^{N}\left(1+\frac{|g_n|^2 d^2}{4\sigma^2\sin^2\theta}\right)}\right] = \underbrace{\iiint\cdots\int}_{\mathrm{N-D\ integral}}\frac{(1+\sum_{n=1}^{N}t_n)^N}{\prod_{n=1}^{N}\left(1+\frac{t_n d^2}{4\sigma^2\sin^2\theta}\right)}\exp(-t_1-t_2-\cdots-t_N)\mathrm{d}t_1\mathrm{d}t_2\cdots\mathrm{d}t_N \tag{A.7}$$

Since we only care about the dominant term in the diversity function of the system, therefore we could expand $(1+\sum_{i=1}^{N}t_k)^N$ in partial fraction polynomial series as

$$(1+\sum_{n=1}^{N}t_n)^N = 1+N\sum_{n=1}^{N}t_n+\cdots \tag{A.8}$$

High order of t_n could only result higher order diversity gain. Therefore, we only keep

the constant component and calculate the diversity function.

$$
\begin{aligned}
&\underbrace{\iiint\cdots\int}_{\mathrm{N-D\ integral}} \frac{(1+\sum_{n=1}^{N} t_n)^N}{\prod_{n=1}^{N}\left(1+\frac{t_k d^2}{4\sigma^2\sin^2\theta}\right)} \exp(-t_1)\exp(-t_2)\cdots\exp(-t_N)\mathrm{d}t_1\mathrm{d}t_2\cdots\mathrm{d}t_N \\
&= \underbrace{\iiint\cdots\int}_{\mathrm{N-D\ integral}} \frac{1}{\prod_{n=1}^{N} 1+\frac{t_n d^2}{4\sigma^2\sin^2\theta}} \exp(-t_1)\exp(-t_2)\cdots\exp(-t_N)\mathrm{d}t_1\mathrm{d}t_2\cdots\mathrm{d}t_N + \mathcal{O}\left(\frac{\ln^{N-1}\rho}{\rho^N}\right) \\
&= \left(\int_0^{\infty} \frac{1}{1+\frac{td^2}{4\sigma^2\sin^2\theta}} \exp(-t)\mathrm{d}t\right)^N + \mathcal{O}\left(\frac{\ln^{N-1}\rho}{\rho^N}\right) \\
&= \left(\frac{4\sigma^2\sin^2\theta}{d^2}\int_{\frac{4\sigma^2\sin^2\theta}{d^2}}^{+\infty} \frac{\exp(-t)\exp(\frac{4\sigma^2\sin^2\theta}{d^2})}{t}\mathrm{d}t\right)^N + \mathcal{O}\left(\frac{\ln^{N-1}\rho}{\rho^N}\right) \\
&= \left(\frac{2(M-1)\sin^2\theta}{3\rho}\left(\mathrm{C}+\ln\rho+\mathcal{O}(\rho^{-1})\right)\left(1+\mathcal{O}(\rho^{-1})\right)\right)^N + \mathcal{O}\left(\frac{\ln^{N-1}\rho}{\rho^N}\right) \\
&= \left(\frac{2(M-1)\sin^2\theta}{3\rho}\ln\rho\right)^N \mathcal{O}\left(\frac{\ln^{N-1}\rho}{\rho^N}\right)
\end{aligned}
\tag{A.9}
$$

where $\mathcal{O}(\rho^{-n})$ means the order of ρ^{-1} is n, C is the Euler–Mascheroni constant and the Signal to Noise Ratio is defined as $\rho = E_s/\sigma^2$. When deriving the diversity function above, we make use of the *Exponential Integral Function*, i.e. $\mathrm{E}_1(x) = \int_x^{+\infty} \frac{\exp(-t)}{t}\mathrm{d}t = -\mathrm{C} - \ln x + \sum_{k=1}^{\infty} \frac{(-1)^{k+1}x^k}{k\cdot k!}$. By substituting the results above into the SEP expression (A.1), the upper and lower bound of the average SEP $\bar{\mathrm{P}}_{\mathrm{SER}}$ can be represented as

$$
\begin{aligned}
\mathrm{P}_1 \leq & \frac{4}{\pi}\left(1-\frac{1}{\sqrt{M}}\right)\int_0^{\frac{\pi}{2}}\left(\frac{2(M-1)\sin^2\theta}{3}\right)^N\left(\frac{\ln\rho}{\rho}\right)^N \mathrm{d}\theta \\
& -\frac{4}{\pi}\left(1-\frac{1}{\sqrt{M}}\right)^2\int_0^{\frac{\pi}{4}}\left(\frac{2(M-1)\sin^2\theta}{3}\right)^N\left(\frac{\ln\rho}{\rho}\right)^N \mathrm{d}\theta \\
& +\mathcal{O}\left(\frac{\ln^{N-1}\rho}{\rho^N}\right) \\
\mathrm{P}_2 = & \frac{4}{\pi}\left(1-\frac{1}{\sqrt{M}}\right)\int_0^{\frac{\pi}{2}}\left(\frac{2(M-1)\sin^2\theta}{3}\right)^N\left(\frac{\ln\rho}{\rho}\right)^N \mathrm{d}\theta \\
& -\frac{4}{\pi}\left(1-\frac{1}{\sqrt{M}}\right)^2\int_0^{\frac{\pi}{4}}\left(\frac{2(M-1)\sin^2\theta}{3}\right)^N\left(\frac{\ln\rho}{\rho}\right)^N \mathrm{d}\theta \\
& +\mathcal{O}\left(\frac{\ln^{N-1}\rho}{\rho^N}\right)
\end{aligned}
\tag{A.10}
$$

From the upper bound and lower bound of SEP, we can verify that the dominate term of the SEP is equivalent and the optimal diversity function can be achieved in the worst case. □

A.2 Proof of Theorem 3

Proof. For component-wise symbol-by-symbol ZF hard detection, the Symbol Error Probability (SEP) fro M-ary square QAM constellation is

$$
\begin{aligned}
P(x_l, f_{j,n}, g_{j,n}) = & \frac{4}{\pi}\left(1-\frac{1}{\sqrt{M}}\right)\int_0^{\frac{\pi}{2}}\exp\left(-\frac{3E_s}{2(M-1)\sigma^2(1+2\sum_{i=1}^N\|\mathbf{g}_i\|^2)[(\boldsymbol{\mathcal{H}}^H\boldsymbol{\mathcal{H}})^{-1}]_{l,l}\sin^2\theta}\right)\mathrm{d}\theta \\
& -\frac{4}{\pi}\left(1-\frac{1}{\sqrt{M}}\right)^2\int_0^{\frac{\pi}{4}}\exp\left(-\frac{3E_s}{2(M-1)\sigma^2(1+2\sum_{i=1}^N\|\mathbf{g}_i\|^2)[(\boldsymbol{\mathcal{H}}^H\boldsymbol{\mathcal{H}})^{-1}]_{l,l}\sin^2\theta}\right)\mathrm{d}\theta
\end{aligned}
\tag{A.11}
$$

The average SEP for all of the symbols can be calculated by taking the arithmetic average of all symbols in $\mathbf{x}'$.

$$P = \frac{1}{L}\sum_{l=1}^{L} P(x_l) \tag{A.12}$$

where $P(x_l)$ is the average SEP of x_l, $P(x_l, f_{j,n}, g_{j,n})$, after taking expectation with respect to $f_{j,n}$ and $g_{j,n}$. Since the negative integral in (A.11) can be reformulated with the first integral and transformed into the addition of two exponential integral expression, we only need to handle the expectation of the exponential integral.

With the inequality introduced in Theorem 3, the SEP of all symbols can be bounded by a single upper limit, so is the arithmetic mean. In order to make the expression clearer, we denote the exponential expression in the integral in (A.11) as $exp(x_l, f_{i,n}, g_{i,n})$. From Lemma 3, the exponential expression has a upper bound of

$$\begin{aligned} exp(x_l, f_{i,n}, g_{i,n}) &= \exp\left(-\frac{3E_s}{2(M-1)\sigma^2(1+2\sum_{i=1}^{N}\|\mathbf{g}_i\|^2)[(\boldsymbol{\mathcal{H}}^H\boldsymbol{\mathcal{H}})^{-1}]_{l,l}\sin^2\theta}\right) \\ &\leq \exp\left(-\frac{aC_0\left\{\sum_{i=1}^{N}\|\mathbf{g}_i\|^2\|\mathbf{f}_i\|^2\right\}}{2\left(1+2\sum_{i=1}^{N}\|\mathbf{g}_i\|^2\right)}\right). \end{aligned} \tag{A.13}$$

where $a = \frac{3E_s}{(M-1)\sin^2\theta}$. The next step is to take the expectation over all the channel coefficients $f_{i,n}$ and $g_{i,n}, i = 1, 2, \cdots, N, n = 1, 2$. As we have assumed before, the channel coefficients are complex circular symmetric Gaussian variables with unit variance. Therefore, the norm squares $\|\mathbf{g}_i\|^2 = |g_{i,1}|^2 + |g_{i,2}|^2$ and $\|\mathbf{f}_i\|^2 = |f_{i,1}|^2 + |f_{i,2}|^2$ are χ_4^2 distributed with the probability density function (pdf) of $p(x) = x\exp(x)$. The expectation with respect to $f_{i,n}$ is calculated in the following expression. Since the

channel realizations are independent, the expectation can be obtained separately.

$$
\begin{aligned}
exp(x_l, g_{i,n}) &= \mathbb{E}_{f_{i,n}}[exp(x_l, f_{i,n}, g_{i,n})] \\
&= \prod_{i=1}^{N} \mathbb{E}_{\mathbf{f}_i} \left[\exp\left(-\frac{aC_0 \|\mathbf{g}_i\|^2 \|\mathbf{f}_i\|^2}{2\left(1 + 2\sum_{i=1}^{N} \|\mathbf{g}_i\|^2\right)} \right) \right] \\
&= \prod_{i=1}^{N} \int_0^{\infty} x_i \exp\left(-\frac{aC_0 \|\mathbf{g}_i\|^2 x_i}{2\left(1 + 2\sum_{i=1}^{N} \|\mathbf{g}_i\|^2\right)} - x_i \right) \mathrm{d}x_i \\
&= \prod_{i=1}^{N} \left(1 + \frac{aC_0 \|\mathbf{g}_i\|^2}{2\left(1 + 2\sum_{i=1}^{N} \|\mathbf{g}_i\|^2\right)} \right)^{-2} \\
&= \prod_{i=1}^{N} \frac{\left(1 + 2\sum_{i=1}^{N} \|\mathbf{g}_i\|^2\right)^2}{\left(1 + 2\sum_{i=1}^{N} \|\mathbf{g}_i\|^2 + \frac{aC_0 \|\mathbf{g}_i\|^2}{2}\right)^2} \\
&\leq \prod_{i=1}^{N} \frac{\left(1 + 2\sum_{i=1}^{N} \|\mathbf{g}_i\|^2\right)^2}{\left(1 + \frac{aC_0 \|\mathbf{g}_i\|^2}{2}\right)^2}
\end{aligned}
\tag{A.14}
$$

In the following steps, the exponential is averaged with respect to $g_{i,n}$.

$$
\begin{aligned}
exp(x_l) = \mathbb{E}_{\mathbf{g}_i}[exp(x_l, g_{i,n})] &= \underbrace{\iiint \cdots \int}_{\text{N-D integral}} \prod_{i=1}^{N} \frac{\left(1 + 2\sum_{i=1}^{N} \|\mathbf{g}_i\|^2\right)^2}{\left(1 + \frac{aC_0 \|\mathbf{g}_i\|^2}{2}\right)^2} x_i \exp(-x_i) \mathrm{d}x_i \\
&= \underbrace{\iiint \cdots \int}_{\text{N-D integral}} \prod_{i=1}^{N} \frac{x_i \exp(-x_i)}{\left(1 + \frac{aC_0 x_i}{2}\right)^2} \mathrm{d}x_i + \mathcal{O}\left(\frac{\ln^N \rho}{\rho^{3N}}\right) \\
&= \left[\int_0^{\infty} \frac{x_i \exp(-x_i)}{\left(1 + \frac{aC_0 x_i}{2}\right)^2} \mathrm{d}x_i \right]^N + \mathcal{O}\left(\frac{\ln^N \rho}{\rho^{3N}}\right)
\end{aligned}
\tag{A.15}
$$

In the integral above, the higher orders of x_i in $\left(1+2\sum_{i=1}^{N}\|\mathbf{g}_i\|^2\right)^2$ will finally results in higher diversity order, thus ignored. Because the lowest diversity order will dominate the SEP performance, high order epxressions can be eliminated from the calculation process. Besides, due to the fact that the symbols transmitted are randomly chosen from the M-ary square QAM constellation with equal probability. the N-dimensional integral can be computed independently.

$$\begin{aligned}
&\int_0^\infty \frac{x_i\exp(-x_i)}{\left(1+\frac{aC_0x_i}{2}\right)^2}\mathrm{d}x_i = \frac{4}{a^2C_0^2}\int_0^\infty \frac{x_i\exp(-x_i)}{\left(x_i+\frac{2}{aC_0}\right)^2}\mathrm{d}x_i \\
=&\frac{4}{a^2C_0^2}\int_0^\infty \frac{\left(x_i+\frac{2}{aC_0}-\frac{2}{aC_0}\right)\exp(-x_i)}{\left(x_i+\frac{2}{aC_0}\right)^2}\mathrm{d}x_i \\
=&\frac{4}{a^2C_0^2}\int_0^\infty \frac{\exp(-x_i)}{\left(x_i+\frac{2}{aC_0}\right)}\mathrm{d}x_i - \frac{8}{a^3C_0^3}\int_0^\infty \frac{\exp(-x_i)}{\left(x_i+\frac{2}{aC_0}\right)^2}\mathrm{d}x_i \\
=&\frac{4}{a^2C_0^2}\left[\left(-\gamma-\ln\frac{2}{aC_0}+\mathcal{O}(\rho^{-1})\right)\exp\left(\frac{2}{aC_0}\right)-\frac{2}{aC_0}\int_0^\infty \frac{\exp(-x_i)}{\left(x_i+\frac{2}{aC_0}\right)^2}\mathrm{d}x_i\right]
\end{aligned} \tag{A.16}$$

where $\gamma = 0.57721$ is the Euler-Mascheroni constant. When deriving the diversity function above, we make use of the *Exponential Integral Function*, i.e. $\mathrm{E}_1(x) =$

$\int_x^{+\infty} \frac{\exp(-t)}{t}\mathrm{d}t = -\gamma - \ln x + \sum_{k=1}^{\infty} \frac{(-1)^{k+1}x^k}{k\cdot k!}$.

$$\begin{aligned}
&\int_0^{\infty} \frac{\exp(-x_i)}{\left(x_i + \frac{2}{aC_0}\right)^2}\mathrm{d}x_i = -\int_0^{\infty} \exp(-x_i)\mathrm{d}\left(\frac{1}{x_i + \frac{2}{aC_0}}\right) \\
=&\exp(-x_i)\frac{1}{x_i + \frac{2}{aC_0}}\Bigg|_0^{\infty} - \int_0^{\infty} \frac{\exp(-x_i)}{\left(x_i + \frac{2}{aC_0}\right)}\mathrm{d}x_i \\
=&\frac{aC_0}{2} - \left(-\gamma - \ln\frac{2}{aC_0} + \mathcal{O}(\rho^{-1})\right)\exp\left(\frac{2}{aC_0}\right)
\end{aligned} \tag{A.17}$$

Therefore, the integral $\int_0^{\infty} \frac{x_i \exp(-x_i)}{\left(1+\frac{aC_0x_i}{2}\right)^2}\mathrm{d}x_i$ can be simplified as

$$\begin{aligned}
&\int_0^{\infty} \frac{x_i \exp(-x_i)}{\left(1 + \frac{aC_0x_i}{2}\right)^2}\mathrm{d}x_i \\
=&\frac{4}{a^2C_0^2}\left\{\left(-\gamma - \ln\frac{2}{aC_0} + \mathcal{O}(\rho^{-1})\right)\exp\left(\frac{2}{aC_0}\right) - \frac{2}{aC_0}\left[\frac{aC_0}{2} - \left(-\gamma - \ln\frac{2}{aC_0} + \mathcal{O}(\rho^{-1})\right)\exp\left(\frac{2}{aC_0}\right)\right]\right\} \\
=&\frac{4}{a^2C_0^2}\left\{\left[C' + \ln\rho + \mathcal{O}(\rho^{-1})\right]\left[1 + \mathcal{O}(\rho^{-1})\right] + \left[-1 + \mathcal{O}\left(\frac{\ln\rho}{\rho}\right)\right]\right\} \\
=&\frac{2^2(M-1)^2\sin^4\theta}{3^2C_0^2\rho^2}\left(C' - 1 + \ln\rho + \mathcal{O}\left(\frac{\ln\rho}{\rho}\right)\right) \\
=&\frac{2^2(M-1)^2\sin^4\theta}{3^2C_0^2}\frac{\ln\rho}{\rho^2} + \frac{2^2(M-1)^2(C'-1)\sin^4\theta}{3^2C_0^2}\frac{1}{\rho^2} + \mathcal{O}\left(\frac{\ln\rho}{\rho^3}\right),
\end{aligned} \tag{A.18}$$

where $C' = -\gamma - \ln 2 + \ln C_0 + \ln\frac{3}{(M-1)\sin^2\theta}$. Combining the intermediate results above, the expectation of the exponential function is

$$\begin{aligned}
exp(x_l) =& \left[\frac{2^2(M-1)^2\sin^4\theta}{3^2C_0^2}\frac{\ln\rho}{\rho^2} + \frac{2^2(M-1)^2(C'-1)\sin^4\theta}{3^2C_0^2}\frac{1}{\rho^2} + \mathcal{O}\left(\frac{\ln\rho}{\rho^3}\right)\right]^N \\
=& \sum_{i=1}^{N}\binom{N}{i}\frac{2^{2N}(M-1)^{2N}(C'-1)^{N-i}\sin^{4N}\theta}{3^{2N}C_0^{2N}}\frac{\ln^i\rho}{\rho^{2N}} + \mathcal{O}\left(\frac{\ln^N\rho}{\rho^{3N}}\right),
\end{aligned} \tag{A.19}$$

where $\binom{n}{i} = \frac{n!}{i!\cdot(n-i)!}$ is the binomial coefficient. Therefore, the SEP can be upper bounded by

$$\begin{aligned} P &= \frac{1}{L}\sum_{l=1}^{L} P(x_l) \\ &= \frac{4}{\pi}\left(1-\frac{1}{\sqrt{M}}\right)\int_0^{\frac{\pi}{2}}\left[\sum_{i=1}^{N}\binom{N}{i}\frac{2^{2N}(M-1)^{2N}(C'-1)^{N-i}}{3^{2N}C_0^{2N}}\frac{\ln^i\rho}{\rho^{2N}}\right]\sin^{4N}\theta\mathrm{d}\theta \\ &- \frac{4}{\pi}\left(1-\frac{1}{\sqrt{M}}\right)^2\int_0^{\frac{\pi}{4}}\left[\sum_{i=1}^{N}\binom{N}{i}\frac{2^{2N}(M-1)^{2N}(C'-1)^{N-i}}{3^{2N}C_0^{2N}}\frac{\ln^i\rho}{\rho^{2N}}\right]\sin^{4N}\theta\mathrm{d}\theta \\ &+ \mathcal{O}\left(\frac{\ln^N\rho}{\rho^{3N}}\right) \end{aligned} \tag{A.20}$$

As shown in the SEP expression above, the lowest order in the integral is $\frac{\ln^N\rho}{\rho^{2N}}$. When the SNR is sufficiently large, the $\frac{\ln^i\rho}{\rho^{2N}}$ will converge to the full diversity order $\frac{1}{\rho^{2N}}$, which is the best that can be achieved with $2N$ antennas. □

Bibliography

[1] C. E. Shannon. Two-way communication channels. In *Proc. 4th Berkeley Symp. Math. Statist. and Prob.*, volume 1, pages 611–644, 1961.

[2] E. van der Meulen. A survey of muti-way channels in information theory. *IEEE Trans. Inform. Theory*, 23:1–37, Jan. 1977.

[3] T. M. Cover and A. E. Gamal. Capacity theorems for the relay channel. *IEEE Trans. Inform. Theory*, 25:572–584, Sep. 1979.

[4] A. Sendonaris, E. Erkip, and B. Aazhang. User cooperation diversity — Part I: System description. *IEEE Trans. Comm.*, 51:1927–1938, Nov. 2003.

[5] A. Sendonaris, E. Erkip, and B. Aazhang. User cooperation diversity — Part II: Implementation aspects and performance analysis. *IEEE Trans. Comm.*, 51:1939–1948, Nov. 2003.

[6] K. Azarian, H. El Gamal, and P. Schniter. On the achievable diversity-multiplexing tradeoff in half-duplex cooperative channels. *IEEE Trans. Inform. Theory*, 51:4152–4157, Dec. 2005.

[7] J. N. Laneman, D. N. C. Tse, and G. W. Wornell. Distributed space-time-coded

protocols for exploiting cooperative diversity in wireless netwoks. *IEEE Trans. Inform. Theory*, 49:2415–2425, Oct. 2003.

[8] J. N. Laneman, D. N. C. Tse, and G. W. Wornell. Cooperative diversity in wireless networks: efficient protocols and outage behavior. *IEEE Trans. Inform. Theory*, 49:2062–3080, Dec. 2004.

[9] R. U. Nabar, H. Bölcskei, and F. W. Kneubühler. Fading relay channels: Performance limits and space-time signal design. *IEEE J. Sel. Areas Commun.*, 22:1099–1109, Aug. 2004.

[10] W. Zhang and K. B. Y. Letaief. Bandwidth efficient cooperative diversity for wireless networks. In *Proceedings IEEE Global telecommunication*, pages 2942–2946, Taipei, Taiwan, 2007.

[11] B. Rankov and A. Wittneben. Spectral efficient protocols for half-duplex fading relay channels. *IEEE J. Select. Areas in Commun.*, 25:379–389, Feb. 2007.

[12] Y. Jing and B. Hassibi. Distributed space-time coding in wireless relay networks. *IEEE Trans. on Wireless Commun.*, 5:3524–3536, Dec. 2006.

[13] S. M. Alamouti. A simple transmit diversity scheme for wireless commincations. *IEEE J. Select. Areas Commun*, 16:1451–1458, Oct. 1998.

[14] V. Tarokh, H. Jafarkhani, and A. R. Calderbank. Space-time block codes from orthogonal designs. *IEEE Trans. Inform. Theory*, 45:1456–1467, July. 1999.

[15] O. Tirkkonen and A. Hottinen. Square-matrix embeddable space-time codes for complex signal constellations. *IEEE Trans. Inform. Theory*, 48:1122–1126, Feb. 2002.

[16] X.-B. Liang. Orthogonal designs with maximal rates. *IEEE Trans. Inform. Theory*, 49:2468–2503, Oct. 2003.

[17] Y. Jing and H. Jafarkhani. Using orthogonal and quasi-orthogonal designs in wireless relay networks. *IEEE Trans. Inform. Theory*, 53:4106–4118, Nov. 2007.

[18] Zhihang Yi and Il-Min Kim. Single-symbol ML decodable distributed STBCs for cooperative networks. *IEEE Trans. Inform. Theory*, 53(8):2977 –2985, Aug. 2007.

[19] J. Harshan and B.S. Rajan. High-rate, single-symbol ML decodable precoded DSTBCs for cooperative networks. *IEEE Trans. Inform. Theory*, 55(5):2004 –2015, may 2009.

[20] Jian-Kang Zhang, J. Liu, and Kon Max Wong. Linear toeplitz space time block codes. In *Information Theory, 2005. ISIT 2005. Proceedings. International Symposium on*, pages 1942–1946, 2005.

[21] Yue Shang and Xiang-Gen Xia. Space-time block codes achieving full diversity with linear receivers. *IEEE Trans. Inform. Theory*, 54(10):4528–4547, 2008.

[22] M. Tomlinson. New automatic equaliser employing modulo arithmetic. *Electronics Letters*, 7(5):138–139, 1971.

[23] J.H. Winters. On the capacity of radio communication systems with diversity in a rayleigh fading environment. *IEEE J. Sel. Areas Commun.*, 5(5):871–878, 1987.

[24] J. Salz. Digital transmission over cross-coupled linear channels. *AT&T Technical Journal*, 64(6):1147–1159, July/Aug. 1985.

[25] Gerard J Foschini. Layered space-time architecture for wireless communication in a fading environment when using multi-element antennas. *Bell labs technical journal*, 1(2):41–59, 1996.

[26] Emre Telatar. Capacity of multi-antenna gaussian channels. *European Transactions on Telecommunications*, 10(6):585–595, 1999.

[27] A. Goldsmith, S.A. Jafar, N. Jindal, and S. Vishwanath. Capacity limits of MIMO channels. *IEEE J. Sel. Areas Commun.*, 21(5):684 – 702, june 2003.

[28] Lizhong Zheng and D.N.C. Tse. Diversity and multiplexing: a fundamental tradeoff in multiple-antenna channels. *IEEE Trans. Inform. Theory*, 49(5):1073–1096, 2003.

[29] S. Verdú. *Multiuser Detection*. Cambridge University Press, 1998.

[30] D. A. Shnidman. A generalized nyquist criterion and an optimum linear receiver for a pulse modulation system. *Bell Syst. Tech. J.*, 46(9):2163–2177, Nov. 1967.

[31] D. A. George. Matched filters for interfering signals. *IEEE Trans. Inform. Theory*, 11(1):153–154, Jan. 1965.

[32] N. Wiener. *Extrapolation, Interpolation, and smoothing of stationary Time Series*. Cambridge, MA: MIT Press, 1949.

[33] J.G. Proakis and M. Salehi. *Digital Communications*. McGraw-Hill International Edition. McGraw-Hill Higher Education, 2008.

[34] A. Goldsmith. *Wireless Communications*. Cambridge University Press, 2005.

[35] H. S. Witsenhausen. A determinant maximization problem occurring in the theory of data communication. *SIAM Journal on Applied Mathematics*, 29(3):515–522, Nov. 1975.

[36] V. Tarokh, N. Seshadri, and A.R. Calderbank. Space-time codes for high data rate wireless communication: performance criterion and code construction. *IEEE Trans. Inform. Theory*, 44(2):744 –765, mar 1998.

[37] B. Hassibi and B.M. Hochwald. High-rate codes that are linear in space and time. *IEEE Trans. Inform. Theory*, 48(7):1804 –1824, jul 2002.

[38] H.L. Van Trees. *Detection, Estimation, and Modulation Theory - Part 1*. Detection, Estimation, and Modulation Theory. Wiley, 2004.

[39] G.H. Golub and C.F. Van Loan. *Matrix Computations*. Johns Hopkins Studies in the Mathematical Sciences. Johns Hopkins University Press, 1996.